

Electronic Supplementary Information

Spatiotemporal dynamics of supramolecular polymers by *in situ* quantitative catalyst-free hydroamination

Minghan Tan,^{ab} Masayuki Takeuchi^{*ab} and Atsuro Takai^{*a}

^a Molecular Design and Function Group, National Institute for Materials Science (NIMS),
1-2-1 Sengen, Tsukuba, Ibaraki 305-0047, Japan

^b Department of Materials Science and Engineering, Faculty of Pure and Applied Sciences,
University of Tsukuba, 1-1-1 Tennodai, Tsukuba, Ibaraki 305-8577, Japan

Table of Contents

| | |
|--|----------|
| S1. Experimental Methods | Page S1 |
| S2. Synthesis and Characterization | Page S3 |
| S3. Supporting Data (Fig. S1–S20 and Table S1) | Page S12 |
| S4. Supporting References | Page S35 |

S1. Experimental Methods

Abbreviations of Chemical Names:

| | |
|-------------------|---|
| CHCl ₃ | chloroform |
| CDCl ₃ | chloroform- <i>d</i> |
| THF | tetrahydrofuran |
| DMF | <i>N,N</i> -dimethylformamide |
| TMS | tetramethylsilane (in NMR data) or trimethylsilyl (in others) |
| DEA | diethylamine |

Materials: Unless otherwise noted, all reagents and solvents were purchased from Tokyo Chemical Industry, Sigma-Aldrich, Wako Pure Chemical Industries and Kanto Chemical and used without further purification. Key compounds were purified by a recycling preparative HPLC (LaboACE LC-5060, Japan Analytical Industry Co., Ltd.) equipped with a gel permeation chromatography (GPC) column (JAIGEL-2HH). Analytical GPC was performed in THF at 313 K using a HLC-8320GPC EcoSEC (TOSOH) equipped with a refractive index detector. The number average molecular weight was calculated on the basis of polystyrene calibration.

Nuclear Magnetic Resonance (NMR) Spectroscopy: NMR spectra were recorded on a JEOL ECS-400 spectrometer and analyzed using an Mnova NMR software. Chemical shifts are presented in parts per million from (ppm) relative to solvent peaks (¹H NMR: CHCl₃ at 7.26 ppm and ¹³C NMR: CDCl₃ at 77.16 ppm).^{S1}

Absorption Spectroscopy: UV-vis-NIR absorption spectra were recorded on a JASCO V-670 spectrophotometer and V-630 spectrophotometer using a cuvette of 1.0 cm path. The time course of reactions was recorded with time-interval measurement mode while stirring sample solution at 600 rpm. Temperature-dependent measurements were recorded at 1 K interval.

Atomic Force Microscopy (AFM): AFM measurements were performed on a Bruker Multimode 8. AFM samples were prepared by spin-coating solutions at the rate of 3000 rpm

onto silicon substrates. We carried out measurements at least three points for each sample to ensure reproducibility.

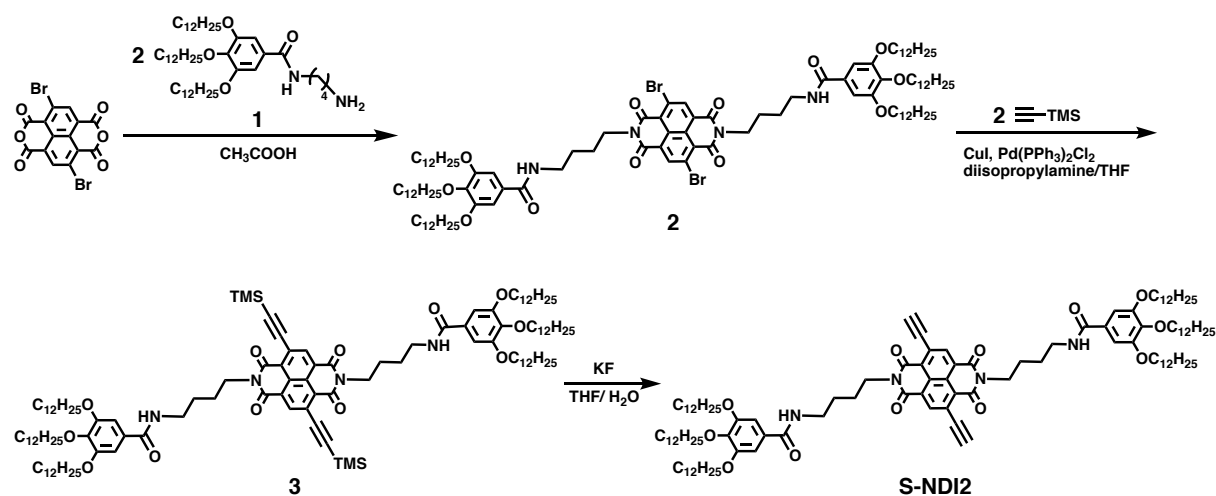
Fourier-Transform Infrared (FT-IR) Spectroscopy: FT-IR spectra were acquired on a JASCO FT/IR 4700 spectrophotometer equipped with an attenuated total reflection (ATR) attachment. The samples were prepared by drying MCH/toluene (4:1 v/v) solutions of **S-NDI2**, **ref-S-NDI** and **S-NDI2-DEA** that were cooled from 363 K to 298 K at the rate of 1 K/min. Prior to the FT-IR measurements, we confirmed that the UV-vis absorption spectrum of each sample was consistent with that in MCH/toluene (4:1 v/v) at 298 K, indicating that the dried sample retained its supramolecular structure. The spectrum of each sample was recorded by 64 scans.

X-ray Diffraction (XRD) Method: XRD patterns were recorded on a Rigaku SmartLab diffractometer equipped with HyPix-3000 X-ray detector. The Cu K α X-ray radiation ($\lambda = 1.5418 \text{ \AA}$) was generated by Cu-rotator anode with operating voltage and current as 45 kV and 200 mA, respectively. The samples were prepared onto non-diffractive silicon plates by drying MCH/toluene (4:1 v/v) solutions of **S-NDI2** and **S-NDI2-DEA** that were cooled from 363 K to 298 K at the rate of 1 K/min. Data were collected in the range of $2\theta = 2^\circ$ to 40° with a scan speed of $2^\circ/\text{min}$ at 298 K. The background (blank) data were subtracted from the raw data.

Mass Spectrometry: Matrix-assisted laser desorption/ionization time-of-flight mass spectrometry (MALDI TOF-MS) was conducted with a Shimadzu AXIMA-CFR Plus, with dithranol as a matrix. Isotopic distribution pattern was calculated using an iMass 1.6 software.

Quantum Chemical Calculation: Computational analysis and graphical representation were carried out with Gaussian 09 software.^{S2} Molecular orbitals of optimized structures were obtained by DFT at the B3LYP/6-31G* level.

S2. Synthesis and Characterization



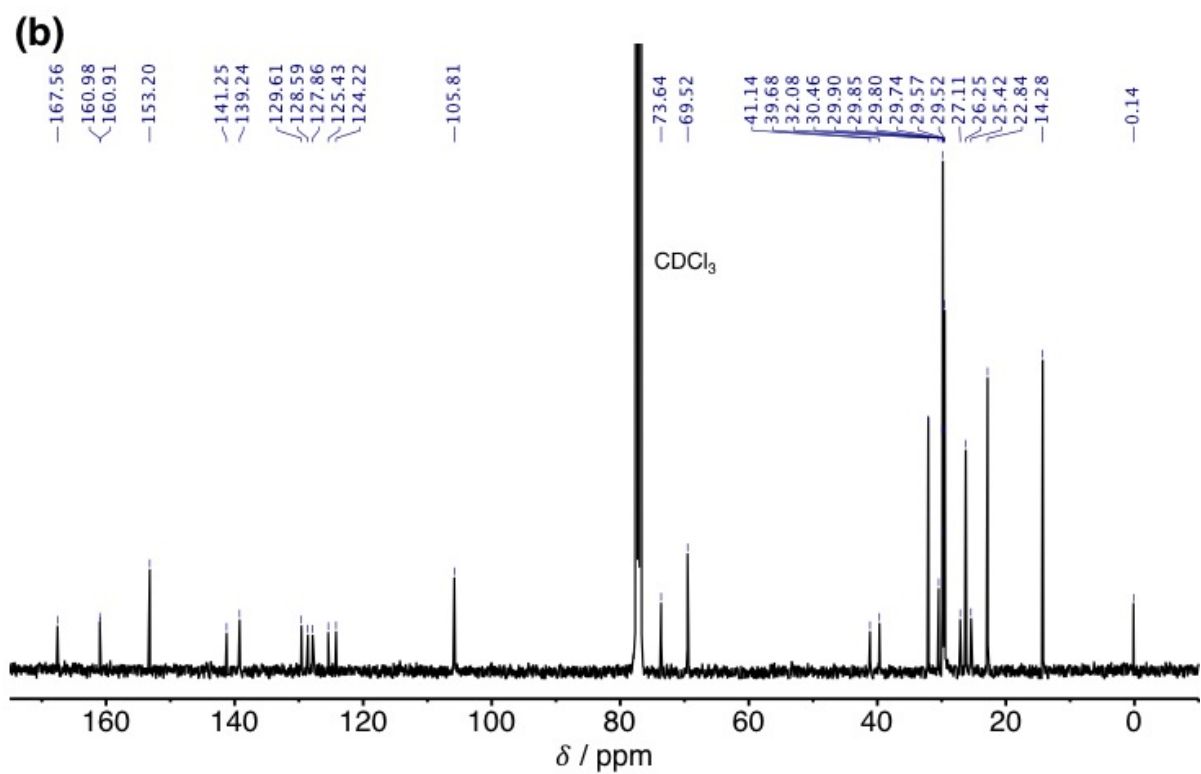
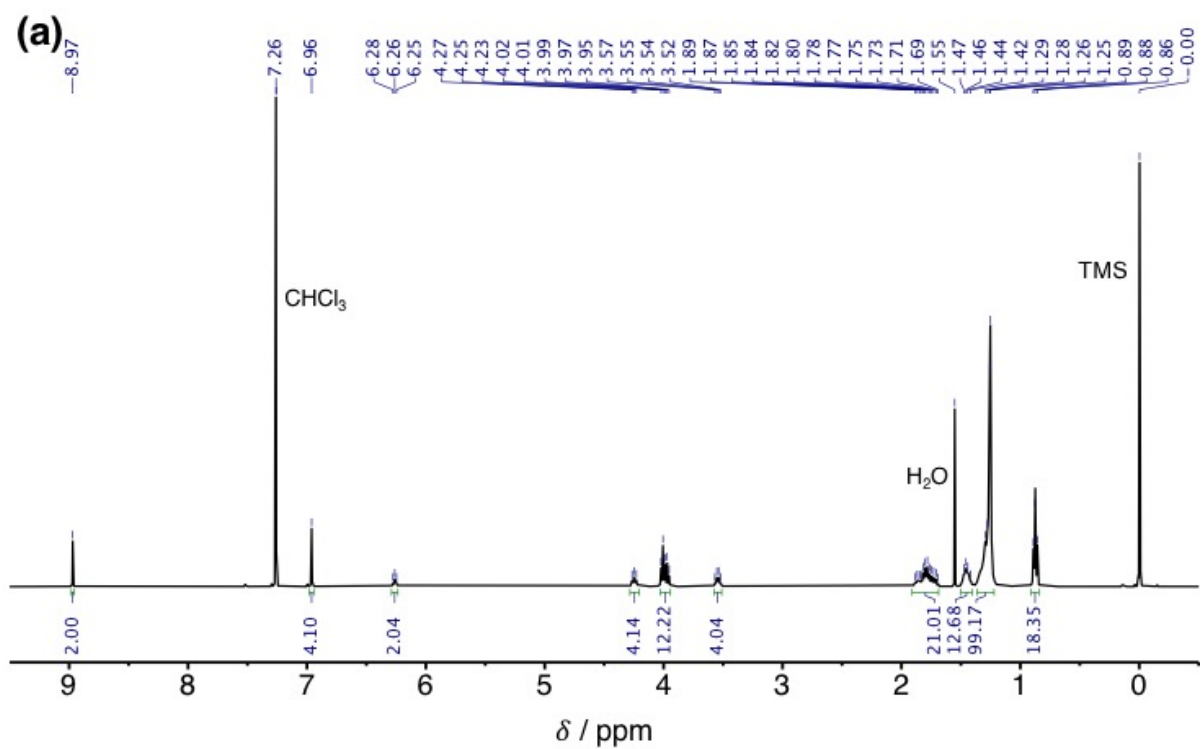
Synthesis of compound **1** was achieved according to the literatures.^{S3-4}

Synthesis of 2: To a 100 mL flask containing 2,6-dibromonaphthalene-1,4,5,8-tetracarboxylic dianhydride (261 mg, 0.61 mmol) and compound **1** (1.0 g, 1.34 mmol) was added 15 mL of acetic acid under N₂ and the mixture was stirred for 1.7 h at reflux. After which, the product was washed by MeOH, filtrated and dried. The residue was further purified from silica gel column chromatography (eluent: CHCl₃/MeOH = 98/2) and reprecipitation from CHCl₃ and MeOH to yield light yellow solid (341 mg, 30%) ¹H NMR (400 MHz, CDCl₃): δ (ppm) = 0.87 (m, 18H), 1.25 (m, 96H), 1.46 (m, 12H), 1.78 (m, 20H), 3.55 (q, J = 6.6 Hz, 4H), 4.00 (m, 12H), 4.25 (t, J = 7.3 Hz, 4H), 6.26 (t, J = 5.9 Hz, 2H), 6.96 (s, 4H), 8.97 (s, 2H). ¹³C NMR (101 MHz, CDCl₃): δ (ppm) = 14.28, 22.84, 25.42, 26.25, 27.11, 29.52, 29.57, 29.74, 29.80, 29.85, 29.90, 30.46, 32.08, 39.68, 41.14, 69.52, 73.64, 105.81, 124.22, 125.43, 127.86, 128.59, 129.61, 139.24, 141.25, 153.20, 160.91, 160.98, 167.56. MALDI TOF-MS (positive ion, reflectron mode): m/z calcd. for C₁₀₈H₁₇₄Br₂N₄O₁₂ [M]⁺ 1877.15; found: 1877.93.

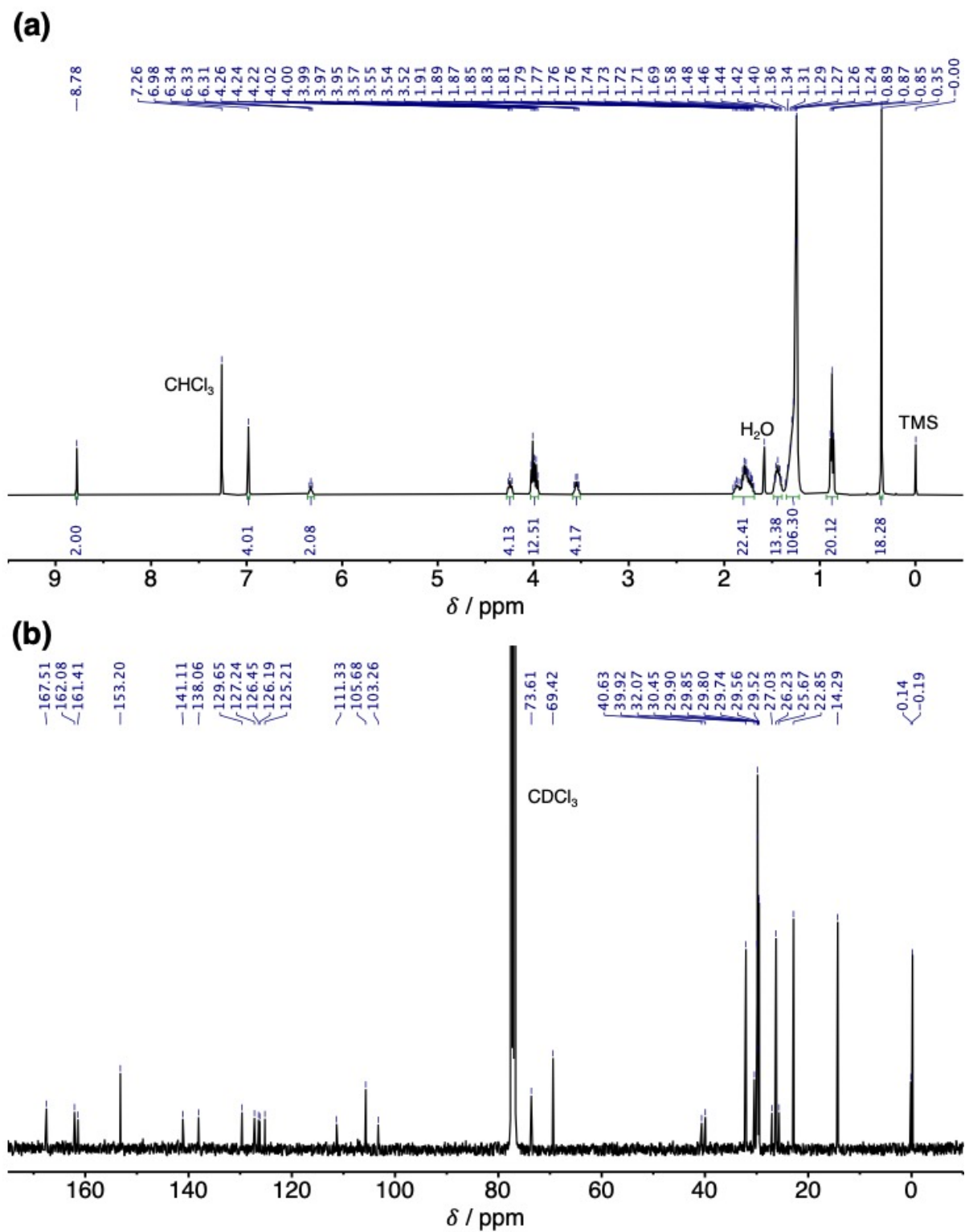
Synthesis of 3: To a 300 mL flask containing **2** (430 mg, 0.23 mmol), CuI (8.6 mg, 45.2 μ mol) and Pd(PPh₃)₂Cl₂ (16.2 mg, 23.1 μ mol) were added 72 mL of dry THF and 21.5 mL of degassed diisopropylamine under N₂ atmosphere. While stirring, trimethylsilylacetylene (170 μ L, 1.23 mmol) was added. The reaction mixture was stirred under N₂ at room temperature for 4.5 h, resulting in dark yellow slurry. Then the mixture was filtered through celite, dried over Na₂SO₄ and solvents were evaporated. The product was further purified by silica gel column chromatography (eluent: CH₂Cl₂/hexane/acetone = 58/39/3) and reprecipitation from CHCl₃ and MeOH to give light yellow solid (188 mg, 43%). ¹H NMR (400 MHz, CDCl₃): δ (ppm) = 0.35 (s, 18H), 0.87 (m, 18H), 1.25 (m, 96H), 1.44 (m, 12H), 1.78 (m, 20H), 3.55 (q, J

= 6.7 Hz, 4H), 4.00 (m, 12H), 4.24 (t, $J = 7.3$ Hz, 4H), 6.33 (t, $J = 5.9$ Hz, 2H), 6.98 (s, 4H), 8.78 (s, 2H). ^{13}C NMR (101 MHz, CDCl_3): δ (ppm) = -0.19, 14.29, 22.85, 25.67, 26.23, 27.03, 29.52, 29.56, 29.74, 29.80, 29.85, 29.90, 30.45, 32.07, 39.92, 40.63, 69.42, 73.61, 103.26, 105.68, 111.33, 125.21, 126.19, 126.45, 127.24, 129.65, 138.06, 141.11, 153.20, 161.41, 162.08, 167.51. MALDI TOF-MS (positive ion, reflectron mode): m/z calcd. for $\text{C}_{118}\text{H}_{192}\text{N}_4\text{O}_{12}\text{Si}_2$ $[\text{M}]^+$ 1913.41; found: 1913.14.

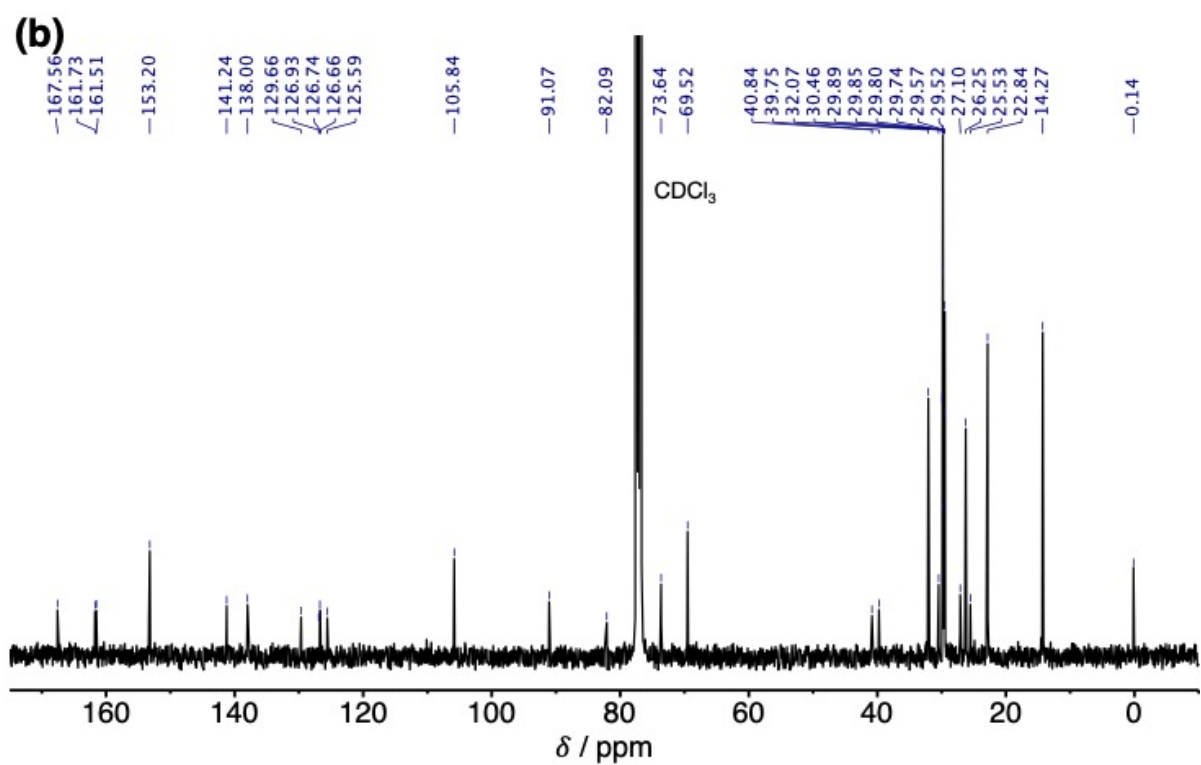
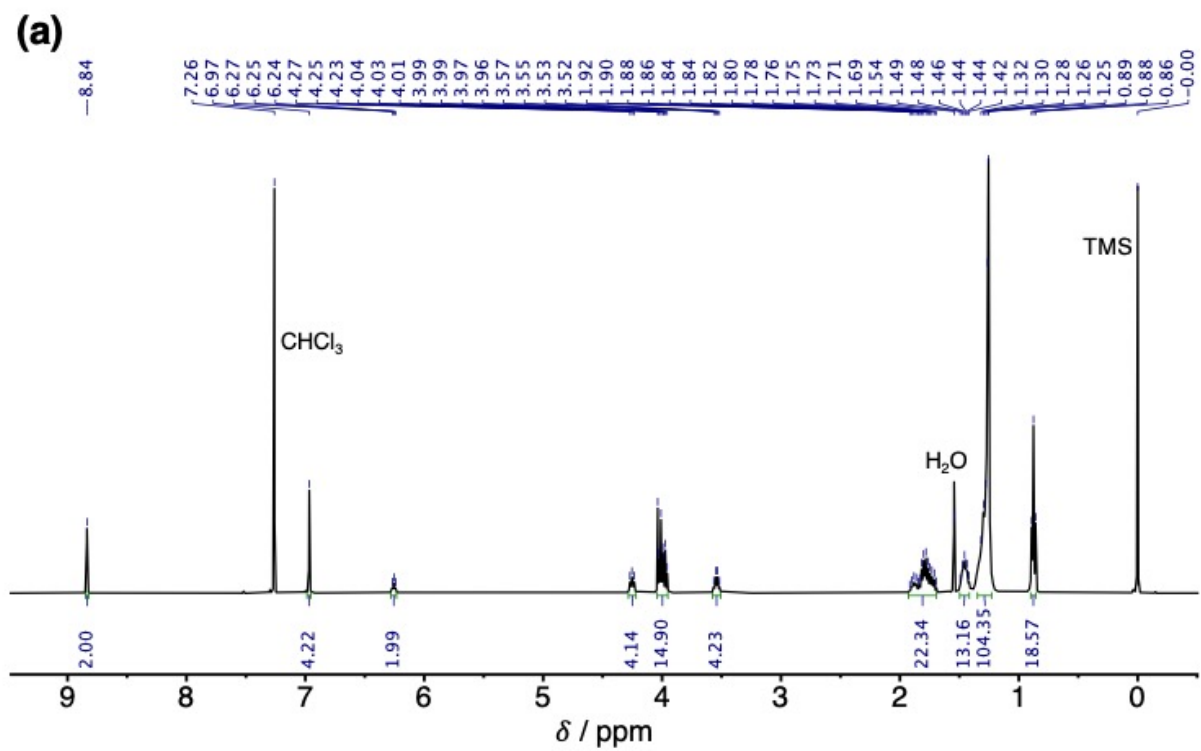
Synthesis of S-NDI2: To a Schlenk flask containing **3** (150 mg, 78.3 μmol) was added 4 mL of dry THF under N_2 atmosphere. An aqueous solution (1 mL) of potassium fluoride (KF, 91 mg, 1.57 mmol) was purged under Ar and then added into flask. The biphasic system was stirred vigorously for 18 h at 35 $^\circ\text{C}$, after which the product was extracted with CHCl_3 , dried over Na_2SO_4 and evaporated. The mixture was further purified by silica gel column chromatography (eluent: CHCl_3 /hexane/acetone = 6/3/1) and reprecipitation from CHCl_3 and MeOH to yield light yellow solid (82 mg, 59%). ^1H NMR (400 MHz, CDCl_3): δ (ppm) = 0.88 (m, 18H), 1.26 (m, 96H), 1.45 (m, 12H), 1.79 (m, 20H), 3.54 (q, $J = 6.5$ Hz, 4H), 4.00 (m, 12H), 4.04 (s, 2H), 4.25 (t, $J = 7.4$ Hz, 4H), 6.26 (t, $J = 5.5$ Hz, 2H), 6.97 (s, 4H), 8.84 (s, 2H). ^{13}C NMR (101 MHz, CDCl_3): δ (ppm) = 14.27, 22.84, 25.53, 26.25, 27.10, 29.52, 29.57, 29.74, 29.80, 29.85, 29.89, 30.46, 32.07, 39.75, 40.84, 69.52, 73.64, 82.09, 91.07, 105.84, 125.59, 126.66, 126.74, 126.93, 129.66, 138.00, 141.24, 153.20, 161.51, 161.73, 167.56. MALDI TOF-MS (positive ion, reflectron mode): m/z calcd. for $\text{C}_{112}\text{H}_{176}\text{N}_4\text{O}_{12}$ $[\text{M}]^+$ 1769.33; found: 1769.21. Elemental analysis (calcd. for $\text{C}_{112}\text{H}_{176}\text{N}_4\text{O}_{12}$: C, 75.97; H, 10.02; N, 3.16): found C, 75.71; H, 9.99; N, 3.16.



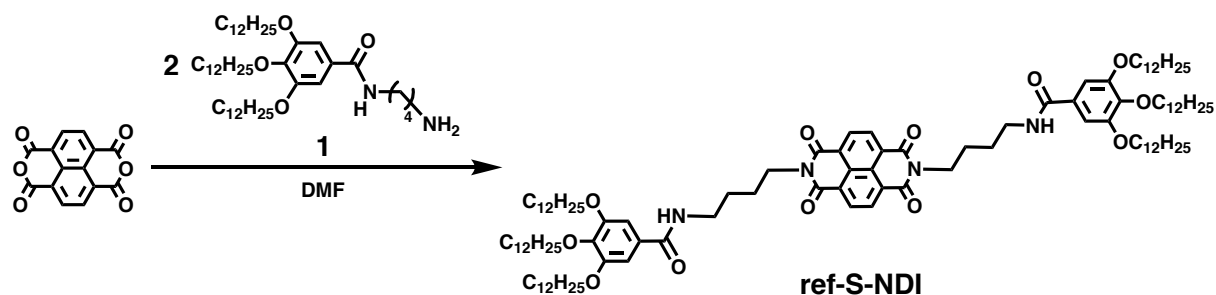
(a) ¹H NMR and (b) ¹³C NMR spectra of **2** in CDCl₃ at 298 K.



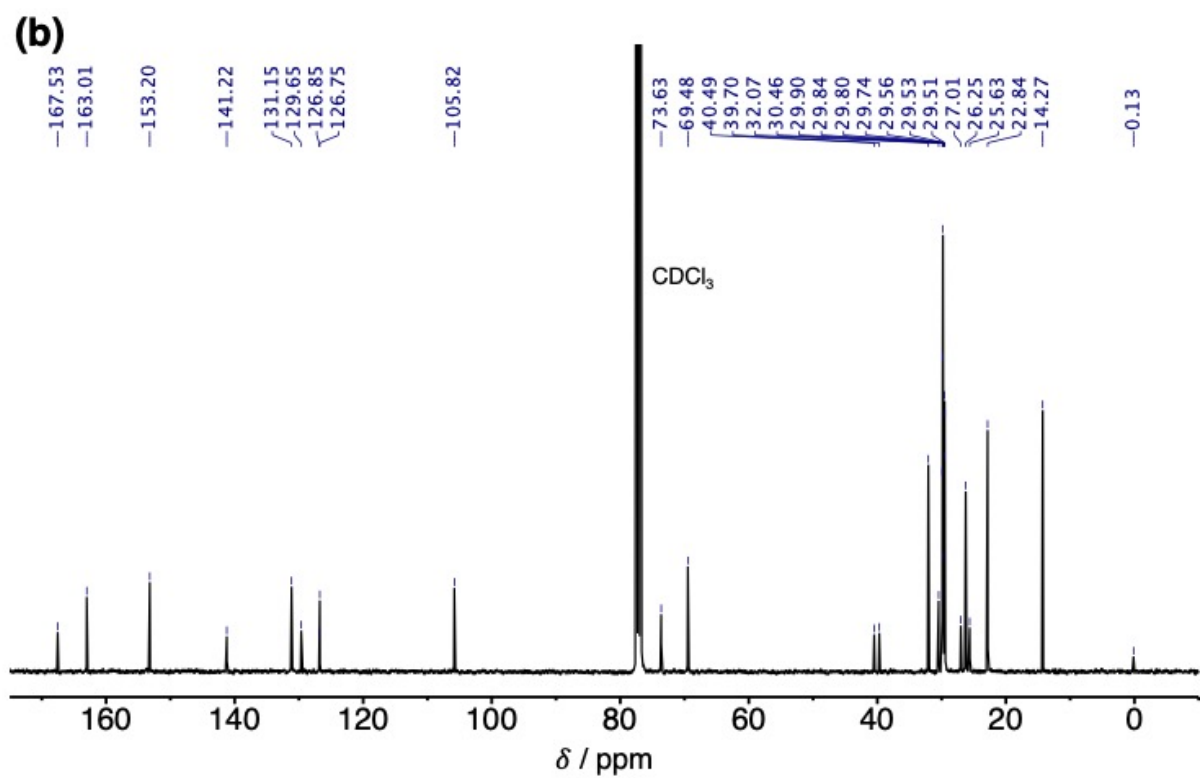
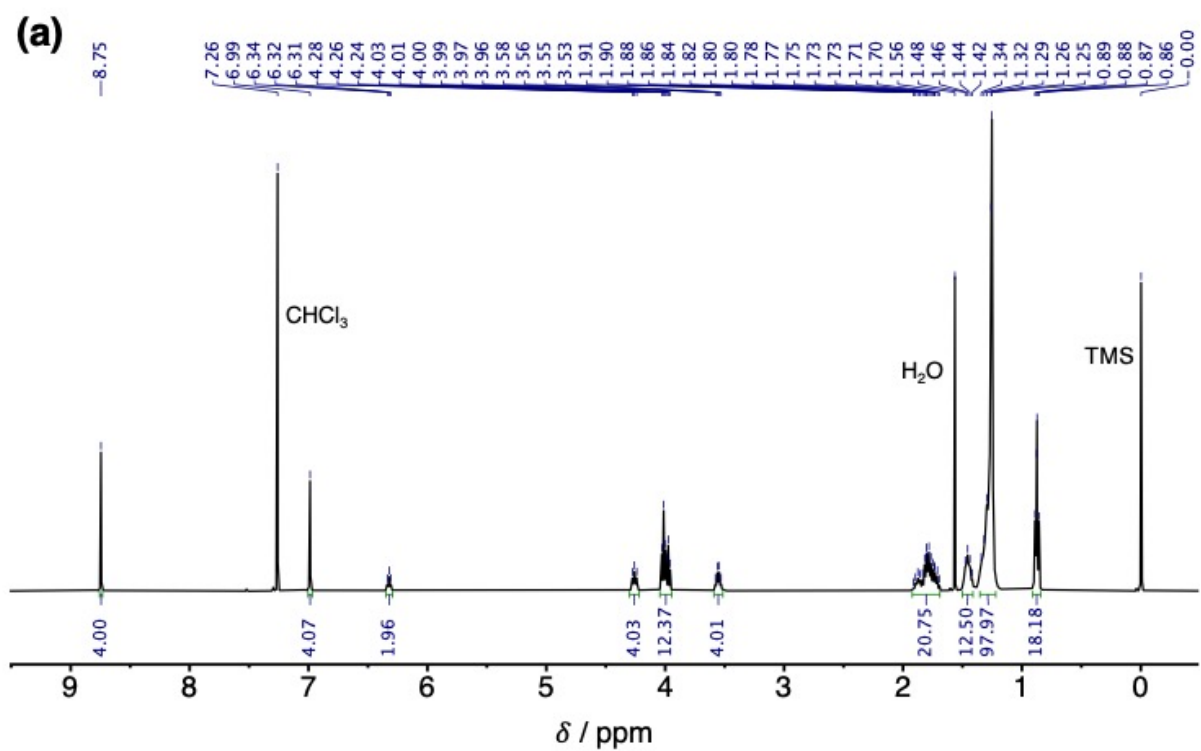
(a) ¹H NMR and (b) ¹³C NMR spectra of **3** in CDCl₃ at 298 K.



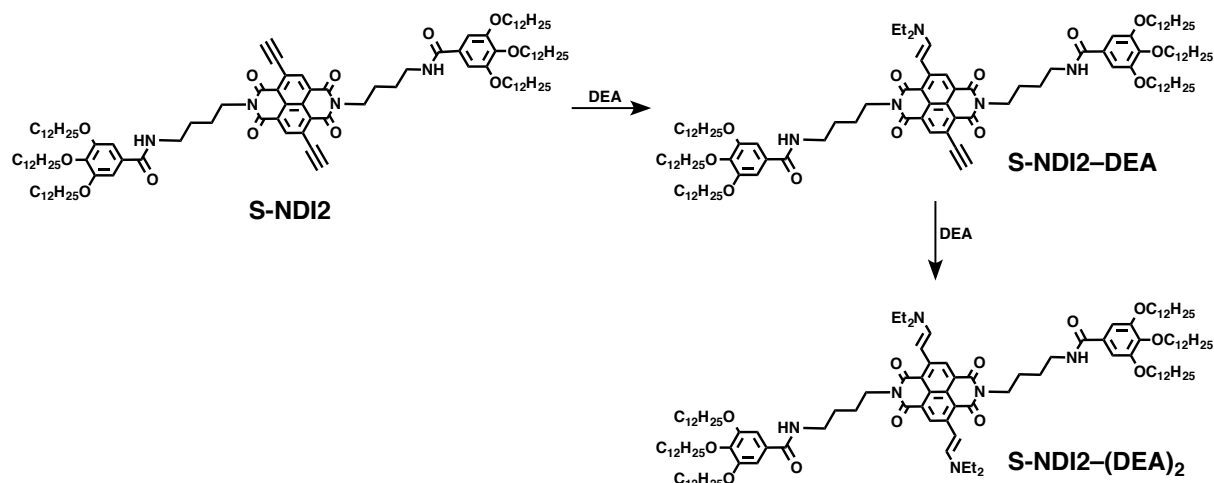
(a) ¹H NMR and (b) ¹³C NMR spectra of **S-NDI2** in CDCl₃ at 298 K.



Synthesis of ref-S-NDI: In a purged flask, 1,4,5,8-naphthalenetetracarboxylic dianhydride (81.8 mg, 0.31 mmol) and compound **1** (501 mg, 0.67 mmol) were dissolved in 15 mL of DMF. The reaction mixture was heated at 145 °C for 5.8 h and cooled in a refrigerator for 30 min. The crude products were collected by filtration, purified by silica gel column chromatography (eluent: CHCl₃/hexane/acetone = 70/27/3) and dried under vacuum to give a cream coloured solid (428 mg, 82%). ¹H NMR (400 MHz, CDCl₃): δ (ppm) = 0.87 (m, 18H), 1.26 (m, 96H), 1.45 (m, 12H), 1.78 (m, 20H), 3.55 (q, *J* = 6.6 Hz, 4H), 3.99 (m, 12H), 4.26 (t, *J* = 7.4 Hz, 4H), 6.33 (t, *J* = 5.9 Hz, 2H), 6.99 (s, 4H), 8.75 (s, 4H). ¹³C NMR (101 MHz, CDCl₃): δ (ppm) = 14.27, 22.84, 25.63, 26.25, 27.01, 29.51, 29.53, 29.56, 29.74, 29.80, 29.84, 29.90, 30.46, 32.07, 39.70, 40.49, 69.48, 73.63, 105.82, 126.75, 126.85, 129.65, 131.15, 141.22, 153.20, 163.01, 167.53. MALDI TOF-MS (positive ion, reflectron mode): *m/z* calcd. for C₁₀₈H₁₇₆N₄O₁₂ [M]⁺ 1721.33; found: 1721.16. Elemental analysis (calcd. for C₁₀₈H₁₇₆N₄O₁₂: C, 75.30; H, 10.30; N, 3.25): found C, 75.31; H, 10.23; N, 3.26.



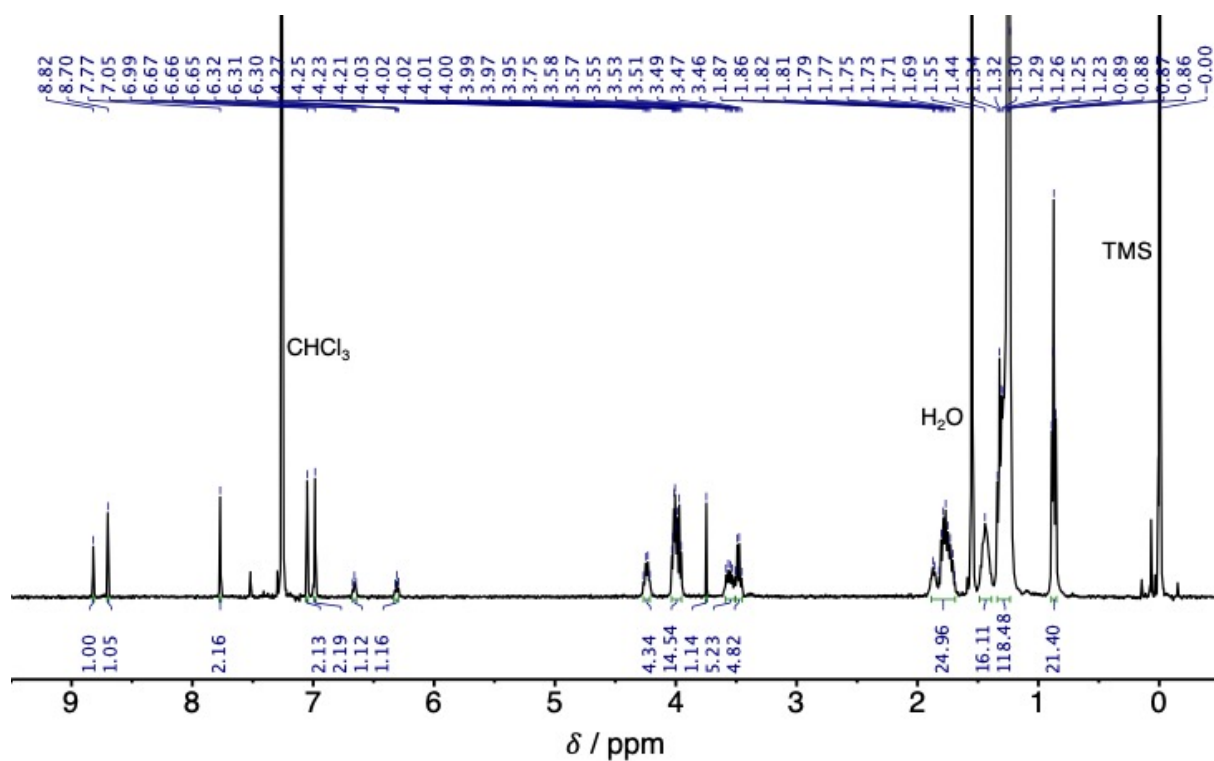
(a) ^1H NMR and (b) ^{13}C NMR spectra of **ref-S-NDI** in CDCl_3 at 298 K.



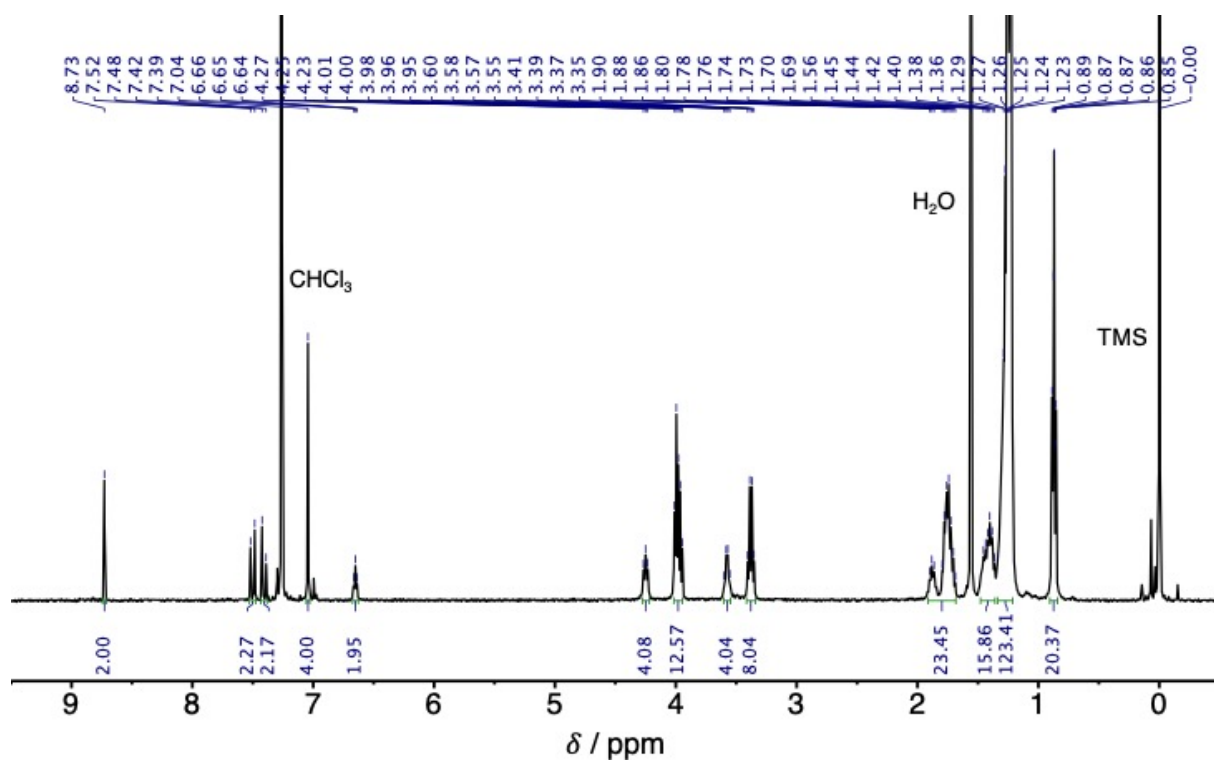
Synthesis of S-NDI2-DEA: To a 50 mL flask containing **S-NDI2** (1.0 mg, 0.56 μmol) was added 5 mL of CHCl_3 under air. Then, diethylamine (**DEA**, 3 μL , 29 μmol) was added and the mixture was stirred for 3.1 h at room temperature. After which, the product was reprecipitated from CHCl_3 and MeOH to yield a dark blue solid, **S-NDI2-DEA** (1.0 mg, 93%). ^1H NMR (400 MHz, CDCl_3): δ (ppm) = 0.87 (m, 18H), 1.26 (m, 102H), 1.44 (m, 12H), 1.79 (m, 20H), 3.48 (q, $J = 7.0$ Hz, 4H), 3.56 (m, 4H), 3.75 (s, 1H), 3.99 (m, 12H), 4.24 (q, $J = 6.8$ Hz, 4H), 6.31 (t, $J = 5.6$ Hz, 1H), 6.66 (t, $J = 5.5$ Hz, 1H), 6.99 (s, 2H), 7.05 (s, 2H), 7.77 (br, 2H), 8.70 (s, 1H), 8.82 (s, 1H). MALDI TOF-MS (positive ion, reflectron mode): m/z calcd. for $\text{C}_{116}\text{H}_{187}\text{N}_5\text{O}_{12}$ $[\text{M}]^+$ 1842.42; found: 1842.23.

It should be noted that the ^1H NMR signal at 7.77 ppm assigned to the olefinic protons of **S-NDI2-DEA** could not be clearly observed at 298 K, but the signal was split into two doublets at lower temperature. The coupling constant was calculated to be 13.3 Hz at 258 K, indicating that **S-NDI2-DEA** was an *E*-isomer.

Synthesis of S-NDI2-(DEA)₂: To a 50 mL flask containing **S-NDI2-DEA** (4.4 mg, 2.4 μmol) was added 5 mL of CHCl_3 under air. Then, **DEA** (0.3 mL, 2.9 mmol) was added and the mixture was stirred for 2.5 h at reflux. After which, the product was reprecipitated from CHCl_3 and MeOH to yield blue green solid (3.3 mg, 72%). ^1H NMR (400 MHz, CDCl_3): δ (ppm) = 0.87 (m, 18H), 1.24 (m, 108H), 1.42 (m, 12H), 1.78 (m, 20H), 3.38 (q, $J = 7.1$ Hz, 8H), 3.58 (q, $J = 6.4$ Hz, 4H), 3.98 (m, 12H), 4.25 (t, $J = 7.3$ Hz, 4H), 6.65 (t, $J = 5.6$ Hz, 2H), 7.04 (s, 4H), 7.41 (d, $J = 13.6$ Hz, 2H), 7.50 (d, $J = 14.0$ Hz, 2H), 8.73 (s, 2H). MALDI TOF-MS (positive ion, reflectron mode): m/z calcd. for $\text{C}_{120}\text{H}_{198}\text{N}_6\text{O}_{12}$ $[\text{M}]^+$ 1915.51; found: 1914.25.



^1H NMR spectrum of **S-NDI2-DEA** in CDCl_3 at 298 K.



^1H NMR spectrum of **S-NDI2-(DEA)₂** in CDCl_3 at 298 K.

S3. Supporting Data

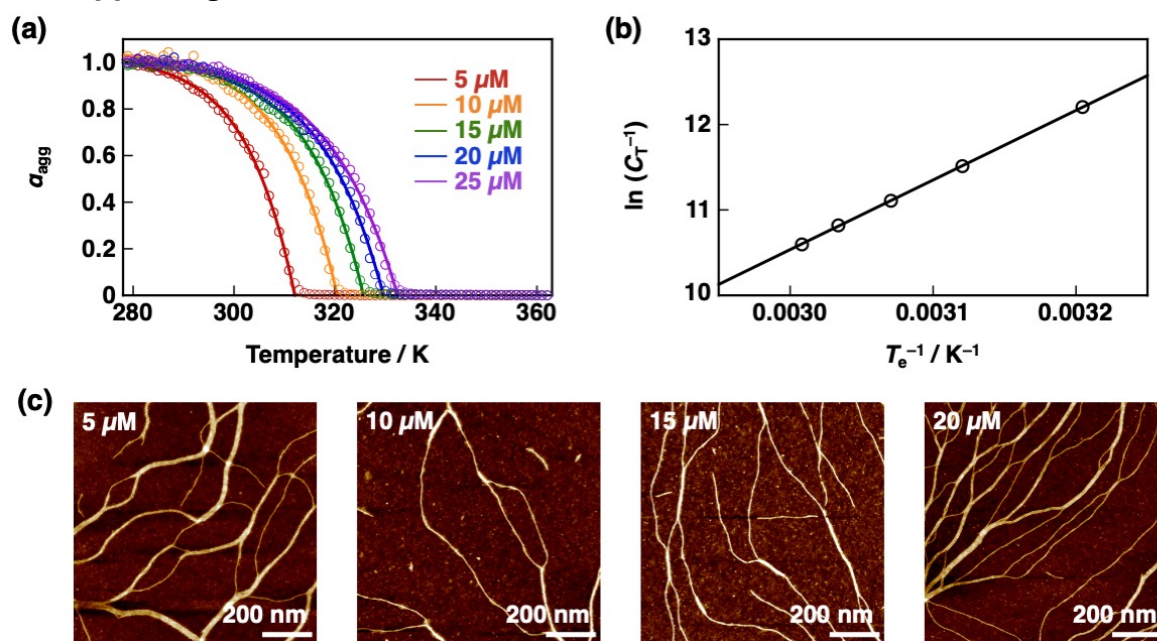


Fig. S1 (a) Plots of degree of polymerization (α_{agg}) of **S-NDI2** versus temperature, calculated from the absorbance at 446 nm at different total concentrations (C_T) in MCH/toluene (4:1 v/v). The solid lines are fitting curves by a cooperative supramolecular polymerization model with R^2 values over 0.99.^{S5} (b) A van't Hoff plot ($\ln C_T^{-1}$ as a function of T_e^{-1}) obtained from the cooling experiment with a linear fit with an R^2 value of 0.999. The standard enthalpy ($-67.8 \text{ kJ mol}^{-1}$) was obtained by multiplying the slope of the linear line by the ideal gas constant, $8.314 \text{ J K}^{-1} \text{ mol}^{-1}$. (c) AFM images of the **S-NDI2** supramolecular polymer spin-coated from MCH/toluene (4:1 v/v) solutions at different C_T . Scale bar: 200 nm.

Table S1 Thermodynamic parameters (α_{SAT} , T_e , ΔH_e) obtained by fitting curves with a cooperative model at different C_T in Fig. S1a

| $C_T / \mu\text{M}$ | α_{SAT} | T_e / K | $\Delta H_e / \text{kJ mol}^{-1}$ |
|---------------------|----------------|------------------|-----------------------------------|
| 5 | 1.028 | 312.1 | -82.9 |
| 10 | 1.051 | 320.5 | -77.9 |
| 15 | 1.010 | 325.7 | -80.2 |
| 20 | 1.025 | 329.6 | -72.3 |
| 25 | 1.031 | 332.4 | -66.8 |

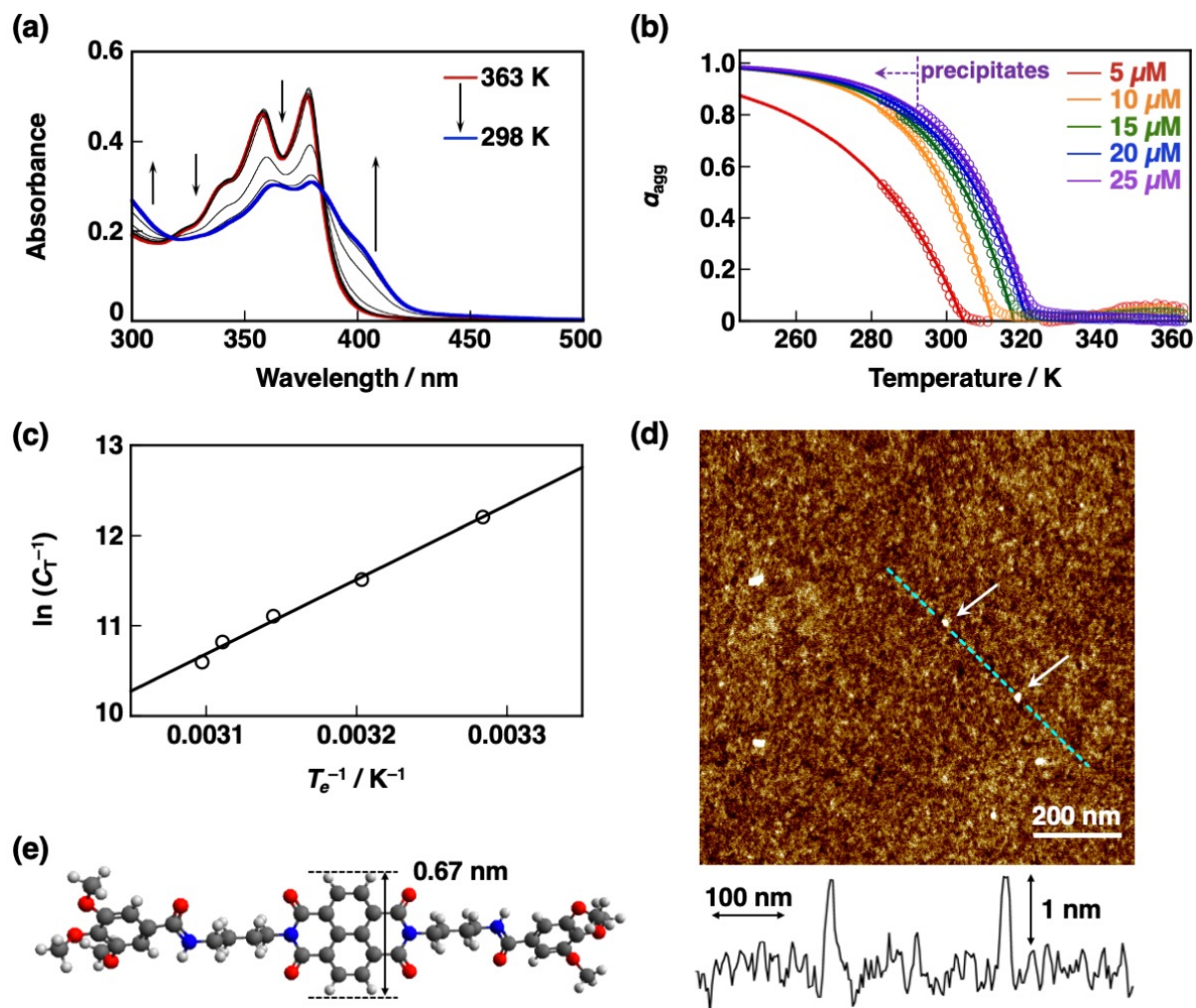


Fig. S2 (a) Temperature-dependent UV-vis absorption spectral changes of **ref-S-NDI** (25 μM) in MCH/toluene (4:1 v/v) upon cooling from 363 K (red line) to 298 K (blue line) at the rate of 1 K/min. (b) Plots of degree of polymerization (α_{agg}) of **ref-S-NDI** versus temperature, calculated from the absorbance at 405 nm at different total concentrations (C_T). The solid lines are fitting curves by a cooperative model with R^2 values over 0.99.^{S5} Note that the formation of precipitates was observed below 298 K at C_T of 25 μM , and the temperature-dependent UV-vis absorption spectra were recorded down to 283 K owing to the instrumental limitations. (c) A van't Hoff plot ($\ln C_T^{-1}$ as a function of T_e^{-1}) obtained from the cooling experiment with a linear fit with an R^2 value of 0.994. The standard enthalpy calculated from the van't Hoff plot is $-68.8 \text{ kJ mol}^{-1}$. (d) AFM image of the supramolecular assembly of **ref-S-NDI** spin-coated from a MCH/toluene (4:1 v/v) solution (top) and its height profile of a cross-section (cyan dashed line, bottom). (e) Optimized structure of **ref-S-NDI** (alkoxy groups, $-\text{OC}_{12}\text{H}_{25}$, were substituted by methoxy group), calculated by DFT at the B3LYP/6-31G* level. Atom colour code: grey, C; red, O; blue, N; white, H.

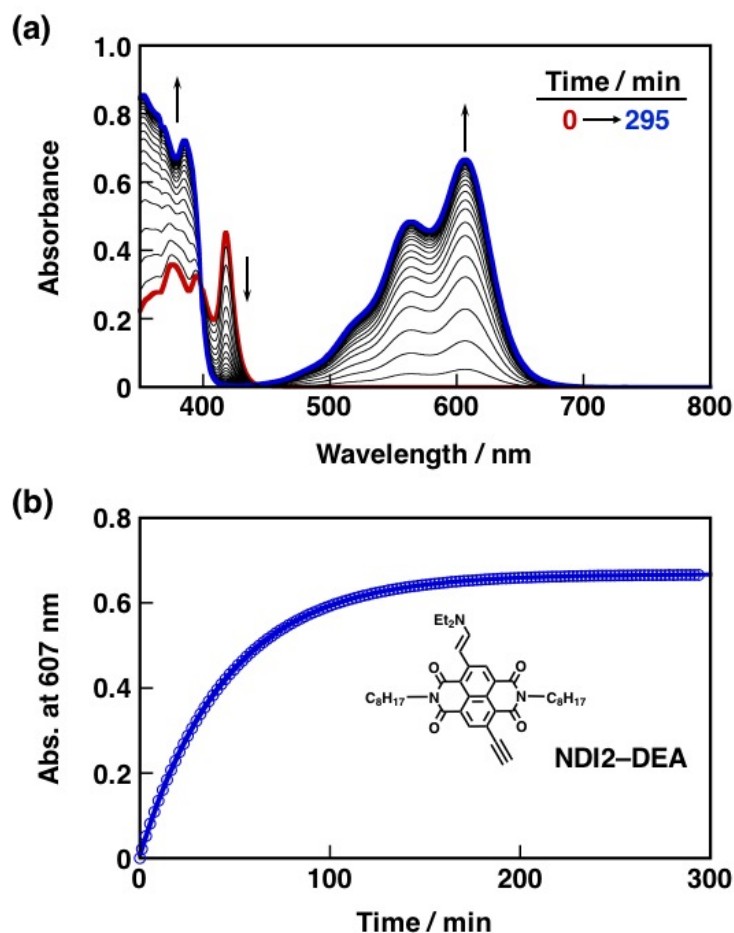


Fig. S3 (a) UV-vis absorption spectral changes observed upon addition of **DEA** (1.24 mM) to a MCH/toluene (4:1 v/v) solution of **NDI2** (25 μM) at 298 K. (b) Time profile of the absorbance change at 607 nm (blue circle), fitted by a pseudo-first-order kinetic curve (blue line) with an R^2 value of 0.999.

The reaction rate of **NDI2** in the presence of excess amine can be described by using eqn S1–S3:

$$d[\text{NDI2-DEA}]/dt = k_{\text{obs}}\{[\text{NDI2}]_0 - [\text{NDI2-DEA}]\} \quad (\text{S1})$$

$$[\text{NDI2-DEA}] = [\text{NDI2}]_0\{1 - \exp(-k_{\text{obs}}t)\} \quad (\text{S2})$$

where k_{obs} (in s^{-1}) is the pseudo-first-order rate constant, defined as $k[\text{DEA}]$, where k (in $\text{M}^{-1}\text{s}^{-1}$) is the second-order rate constant for the formation of an amine monoadduct (**NDI2-DEA**), and $[\text{NDI2}]_0$ is the initial concentration of **NDI2**. Because the absorbance at 607 nm (A_{607}) is derived solely from **NDI2-DEA**, the time course of A_{607} is given by eqn S3:

$$A_{607} = \varepsilon_{607} \times [\text{NDI2}]_0\{1 - \exp(-k_{\text{obs}}t)\} \quad (\text{S3})$$

where ε_{607} is the molar extinction coefficient of **NDI2-DEA** at 607 nm. The time profile of the change in absorbance at 607 nm was fitted well by the pseudo-first-order kinetic curve expressed by eqn S3. The k_{obs} and k values were determined to be $3.65 \times 10^{-4} \text{ s}^{-1}$ and $2.94 \times 10^{-1} \text{ M}^{-1} \text{ s}^{-1}$, respectively.

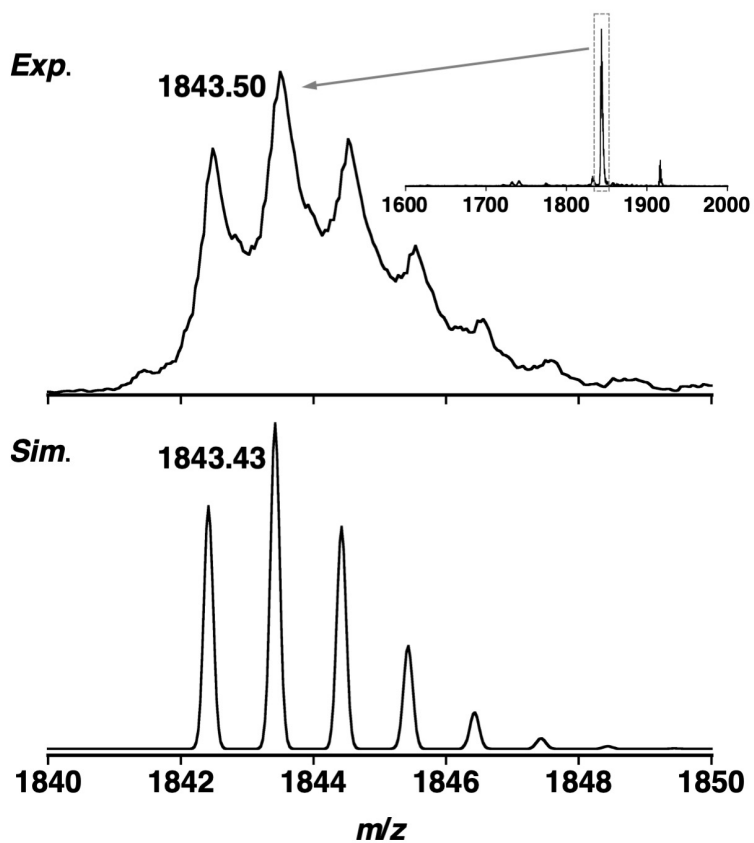
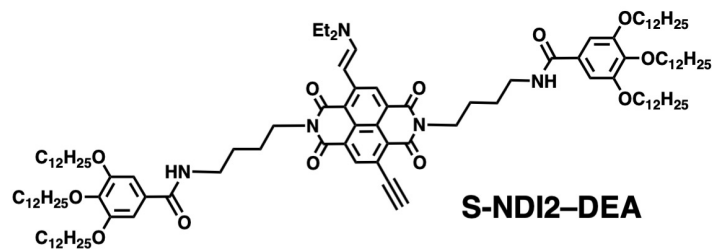


Fig. S4 MALDI TOF-MS (positive ion, reflectron mode) chart obtained 1200 min after the reaction between the **S-NDI2** supramolecular polymer ($C_T = 25 \mu\text{M}$) and **DEA** (1.24 mM) was initiated in MCH/toluene (4:1 v/v) at 298 K and its calculated isotopic distribution (calcd. for $[\text{S-NDI2-DEA}]^+$; $\text{C}_{116}\text{H}_{187}\text{N}_5\text{O}_{12}$).

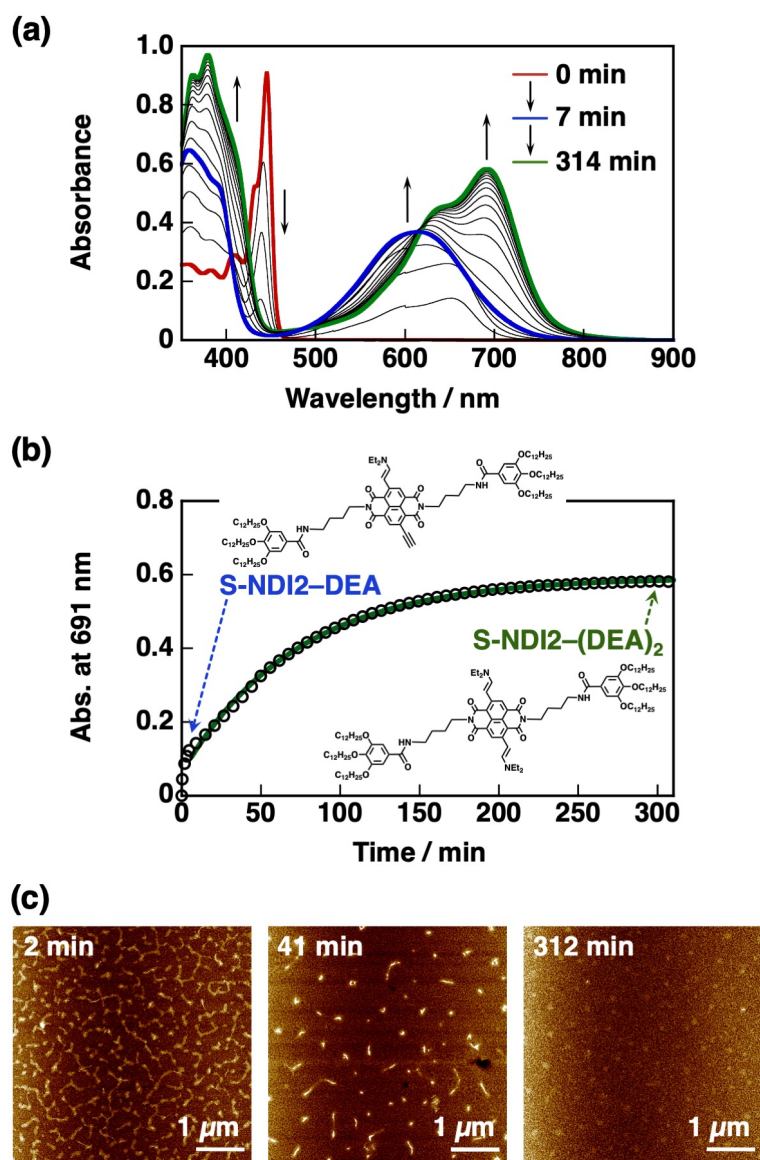


Fig. S5 (a) UV-vis-NIR absorption spectral changes of the **S-NDI2** supramolecular polymer ($C_T = 25 \mu\text{M}$) observed upon addition of **DEA** (159 mM) in MCH/toluene (4:1 v/v) at 298 K. The stepwise absorption spectral changes (red–blue–green lines) indicate the formation of supramolecular assemblies of an amine monoadduct **S-NDI2–DEA** followed by an amine bisadduct **S-NDI2–(DEA)₂**. (b) Time profile of absorbance change at 691 nm during the reaction (black circle). The green solid line shows a pseudo-first-order fitting curve (R^2 values of 0.999) for the second step, namely the formation of the bisadduct. The pseudo-first-order and second-order rate constants were determined to be $k_{\text{obs}} = 2.30 \times 10^{-4} \text{ s}^{-1}$ and $k = 1.44 \times 10^{-3} \text{ M}^{-1} \text{ s}^{-1}$, respectively. (c) AFM images observed during the reaction. Samples were prepared by spin-coating from the MCH/toluene (4:1 v/v) solution at 2 min, 41 min and 312 min after addition of **DEA**. Scale bar: 1 μm .

Based on the second-order rate constants for the formation of **S-NDI2–DEA** ($k = 6.30 \times 10^{-2} \text{ M}^{-1} \text{ s}^{-1}$) and **S-NDI2–(DEA)₂** ($k = 1.44 \times 10^{-3} \text{ M}^{-1} \text{ s}^{-1}$), the corresponding pseudo-first-order rate constants ($k_{\text{obs}} = k[\text{DEA}]$) at 1.24 mM of **[DEA]** can be determined as

$7.81 \times 10^{-5} \text{ M}^{-1} \text{ s}^{-1}$ and $1.78 \times 10^{-6} \text{ M}^{-1} \text{ s}^{-1}$, respectively. The time courses of **[S-NDI2-DEA]** and **[S-NDI2-(DEA)₂]** are expressed by eqn S4 and S5:

$$\text{[S-NDI2-DEA]} = \text{[S-NDI2]}_0 \{1 - \exp(7.81 \times 10^{-5} t)\} \quad (\text{S4})$$

$$\begin{aligned} \text{[S-NDI2-(DEA)}_2\text{]} &= \text{[S-NDI2-DEA]} \{1 - \exp(-1.78 \times 10^{-6} t)\} \\ &= \text{[S-NDI2]}_0 \{1 - \exp(-7.81 \times 10^{-5} t)\} \{1 - \exp(-1.78 \times 10^{-6} t)\} \end{aligned} \quad (\text{S5})$$

where **[S-NDI2]₀** is the initial concentration of **S-NDI2**. The formation of **S-NDI2-(DEA)₂** is much slower than that of **S-NDI2-DEA**; for example, given that **[S-NDI2]₀** is 25 μM , it is estimated that **[S-NDI2-(DEA)₂]** is formed less than 3 μM even 1200 min after the start of the reaction. We therefore infer that the effect of **S-NDI2-(DEA)₂** on the dynamics during the monoadduct formation is not significant.

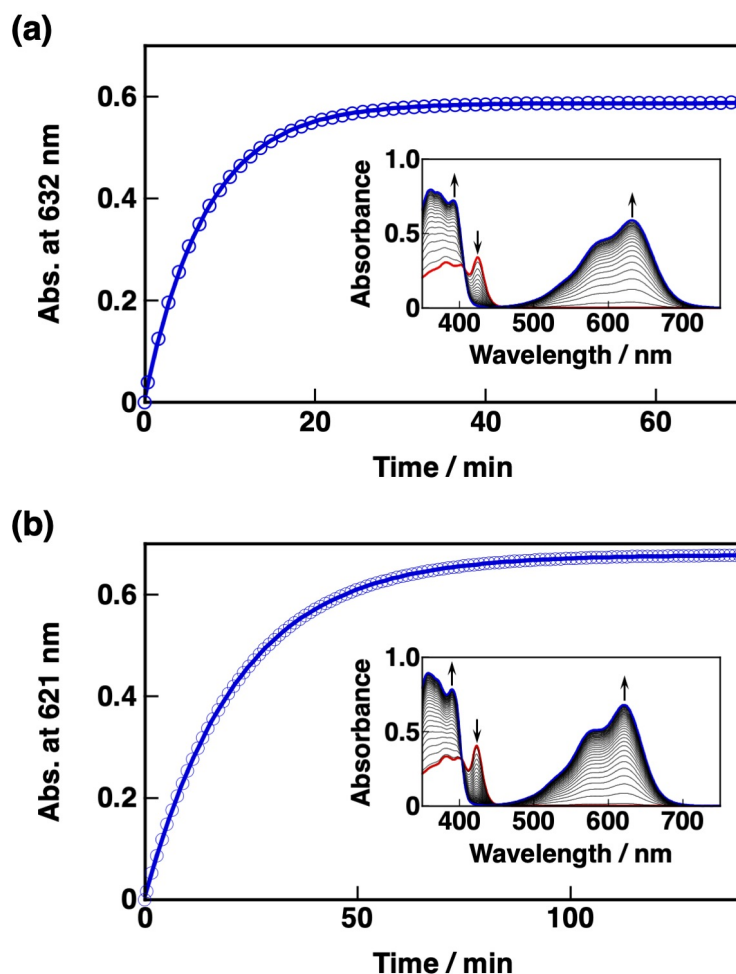


Fig. S6 (a) UV-vis absorption spectral changes of the **S-NDI2** monomer (25 μM) observed upon addition of **DEA** (1.24 mM) in pure toluene at 298 K, and its time profile at 632 nm fitted by a pseudo-first-order kinetic curve (blue line) with an R^2 value of 0.999. Note that **S-NDI2** does not form any supramolecular assemblies under these conditions. (b) UV-vis absorption spectral changes of the **NDI2** monomer (25 μM) observed upon addition of **DEA** (1.24 mM) in toluene at 298 K, and its time profile at 621 nm fitted by a pseudo-first-order kinetic curve (blue line) with an R^2 value of 0.999.

The k_{obs} and k values for the **S-NDI2** monomer were determined to be $2.32 \times 10^{-3} \text{ s}^{-1}$ and $1.87 \text{ M}^{-1} \text{ s}^{-1}$ respectively, while those for the **NDI2** monomer were determined to be $7.68 \times 10^{-4} \text{ s}^{-1}$ and $6.19 \times 10^{-1} \text{ M}^{-1} \text{ s}^{-1}$ respectively. These results indicate that the **S-NDI2** monomer has slightly higher reactivity than the **NDI2** monomer.

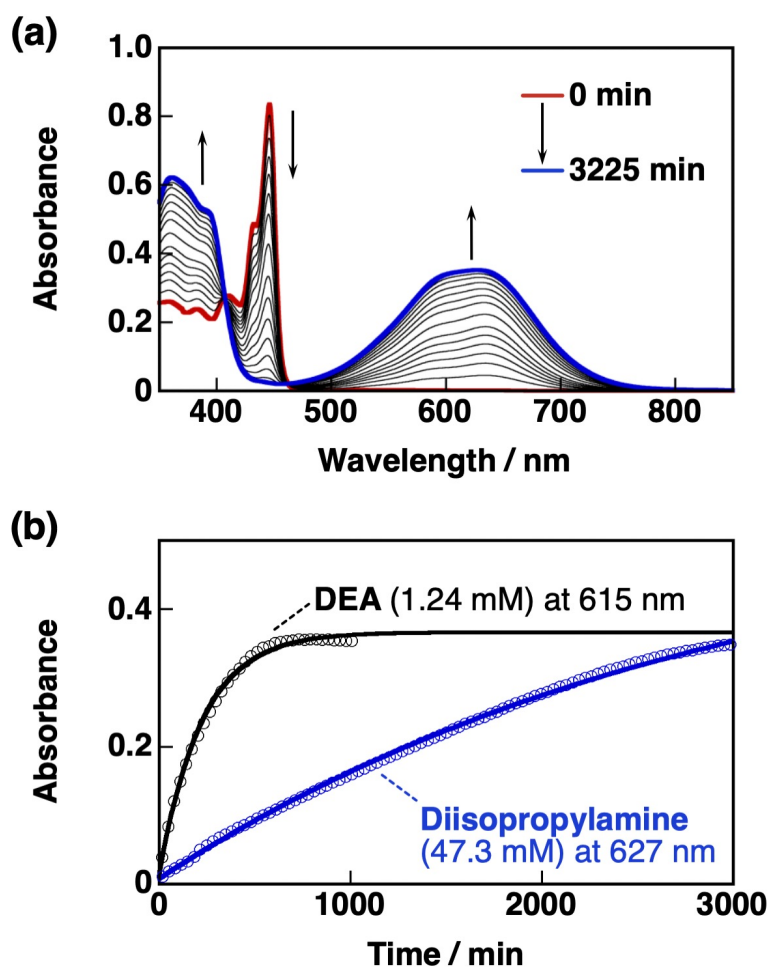


Fig. S7 (a) UV-vis absorption spectral changes of the **S-NDI2** supramolecular polymer ($C_T = 25 \mu\text{M}$) observed upon addition of diisopropylamine (47.3 mM) in MCH/toluene (4:1 v/v) at 298 K. (b) Time profiles of absorbance change during the reaction of the **S-NDI2** supramolecular polymer ($C_T = 25 \mu\text{M}$) with **DEA** (1.24 mM) at 615 nm (black circle) and diisopropylamine (47.3 mM) at 627 nm (blue circle) at 298 K. The k_{obs} values (in s^{-1}) in the reaction with diisopropylamine and **DEA** were determined to be 5.7×10^{-6} and 7.8×10^{-5} , respectively. Thus, the k values (in $\text{M}^{-1} \text{s}^{-1}$) in the reaction with diisopropylamine and **DEA** were 1.2×10^{-4} and 6.3×10^{-2} , respectively.

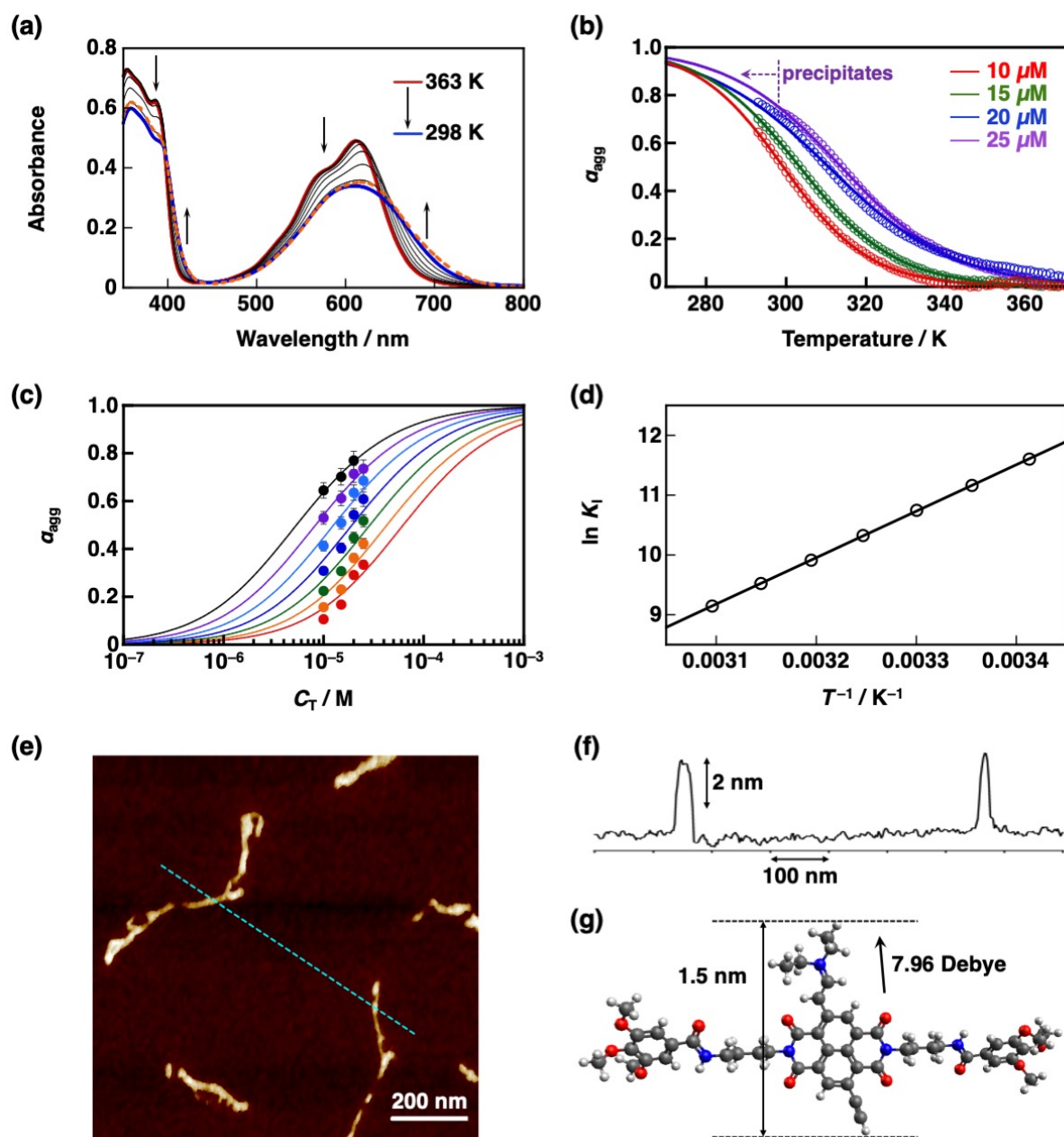


Fig. S8 (a) Temperature-dependent UV-vis absorption spectral changes of **S-NDI2-DEA** (25 μM) in MCH/toluene (4:1 v/v) upon cooling from 363 K (red line) to 298 K (blue line) at the rate of 1 K/min. The orange dotted line is the UV-vis absorption spectrum of the **S-NDI2** supramolecular polymer ($C_T = 25 \mu\text{M}$) 1200 min after the reaction with **DEA** (1.24 mM) in MCH/toluene (4:1 v/v) at 298 K. (b) Plots of degree of polymerization (α_{agg}) of **S-NDI2-DEA** versus temperature, calculated from the absorbance at 700 nm at different C_T . The solid lines are fitting curves with an isodesmic model represented by eqn S6 with R^2 values over 0.997.^{S5} Note that the formation of precipitates was observed below 298 K at C_T of 25 μM . (c) Plots of α_{agg} versus C_T at different temperatures in the range of 293 K to 323 K, fitted by eqn S7 to give aggregation constants (K_I) with R^2 values over 0.9.^{S6,S7} (d) A van't Hoff plot ($\ln K_I$ as a function of T^{-1}) with an R^2 value of 0.999. The standard enthalpy ($-64.6 \text{ kJ mol}^{-1}$) was

obtained by multiplying the slope of the linear line by the ideal gas constant, $8.314 \text{ J K}^{-1} \text{ mol}^{-1}$. (e) AFM image of the supramolecular assembly of **S-NDI2-DEA** spin-coated from a MCH/toluene (4:1 v/v) solution. (f) The height profile of a cross-section (cyan dashed line) in (e). (g) Optimized structure of **S-NDI2-DEA** (alkoxy groups, $-\text{OC}_{12}\text{H}_{25}$, were substituted by methoxy group), calculated by DFT at the B3LYP/6-31G* level. Atom colour code: grey, C; red, O; blue, N; white, H.

Eqn S6 and S7 are represented as follows:

$$\alpha_{\text{agg}} \approx 1/\{1 + \exp(-0.908\Delta H(T-T_m)/RT_m^2)\} \quad (\text{S6})$$

where α_{agg} is estimated from eqn (1), ΔH is an aggregation enthalpy, T is the absolute temperature, T_m is the melting temperature defined as the temperature for which α_{agg} is 0.5 and R is the ideal gas constant.

$$\alpha_{\text{agg}} = 1 - \{2K_I C_T + 1 - (4K_I C_T + 1)^{0.5}\}/(2K_I^2 C_T^2) \quad (\text{S7})$$

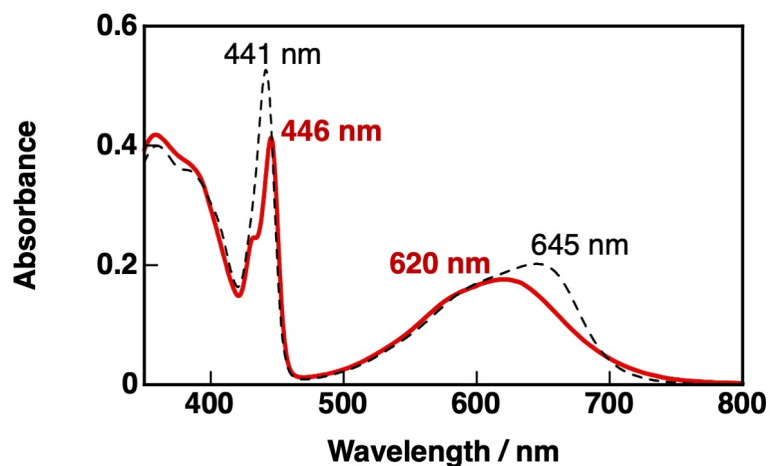


Fig. S9 UV-vis absorption spectrum of a mixture of supramolecular polymers of **S-NDI2** ($C_T = 12.5 \mu\text{M}$) and **S-NDI2-DEA** ($C_T' = 12.5 \mu\text{M}$) in MCH/toluene (4:1 v/v) at 298 K (red solid line). The absorption spectrum did not change over 15 h, and the distinct absorption peaks at 446 nm attributed to **S-NDI2** and at 620 nm attributed to **S-NDI2-DEA** indicated that the two components remained unmixed. The UV-vis absorption spectrum of the intermediate during the *in situ* hydroamination (black dashed line; 150 min after the start of the reaction in Fig. 3a) is clearly different from the red solid line.

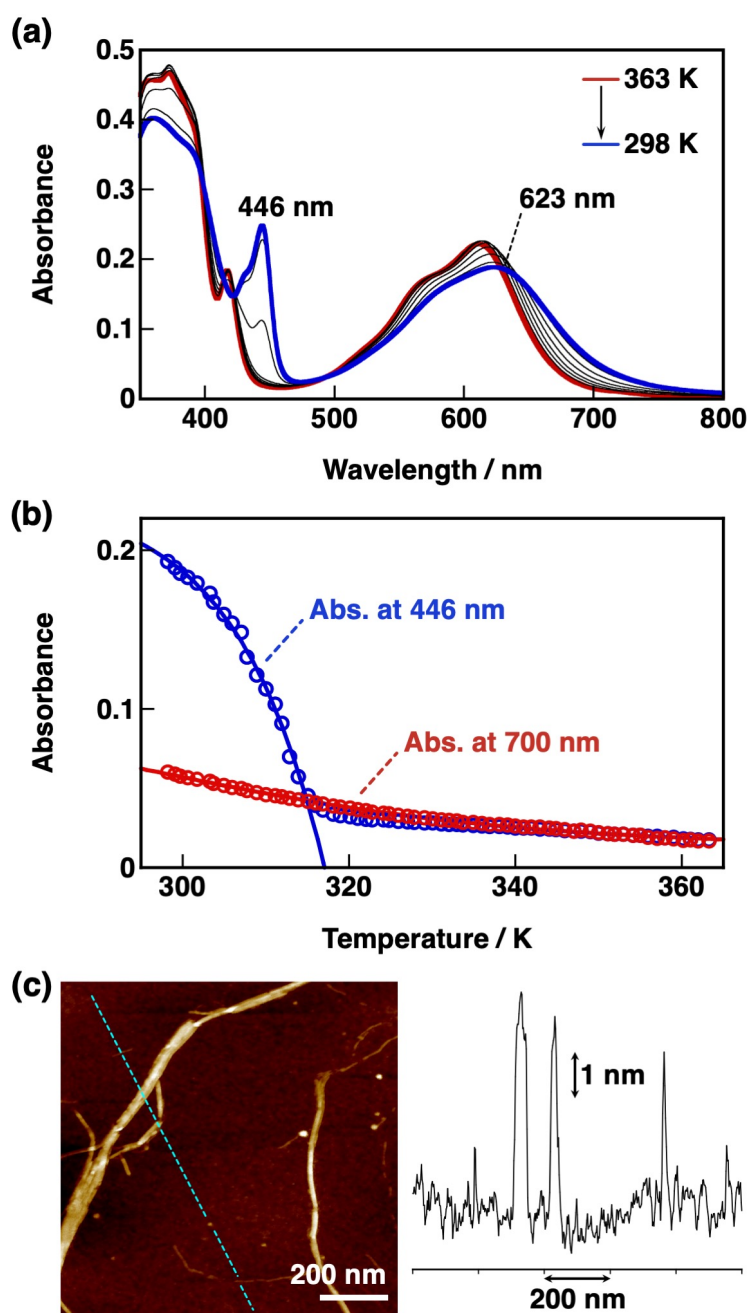


Fig. S10 (a) Temperature-dependent UV-vis absorption spectral changes of **S-NDI2** (12.5 μM) and **S-NDI2-DEA** (12.5 μM) in MCH/toluene (4:1 v/v) upon cooling from 363 K (red line) to 298 K (blue line) at the rate of 1 K/min. The UV-vis absorption spectrum at 298 K showed peaks at 446 nm and 623 nm, indicating the formation of self-sorted supramolecular assemblies of **S-NDI2** and **S-NDI2-DEA**. (b) Plots of the absorbance at 446 nm (blue circle) and at 700 nm (red circle) against temperature, which are fitted by a cooperative model (blue solid line; $T_e = 316$ K) and an isodesmic model (red solid line), respectively. (c) AFM image of the self-sorted assemblies spin-coated from the MCH/toluene (4:1 v/v) solution used for the UV-vis absorption measurement. Scale bar: 200 nm. The height profile of a cross-section (cyan dashed line) is shown on the right.

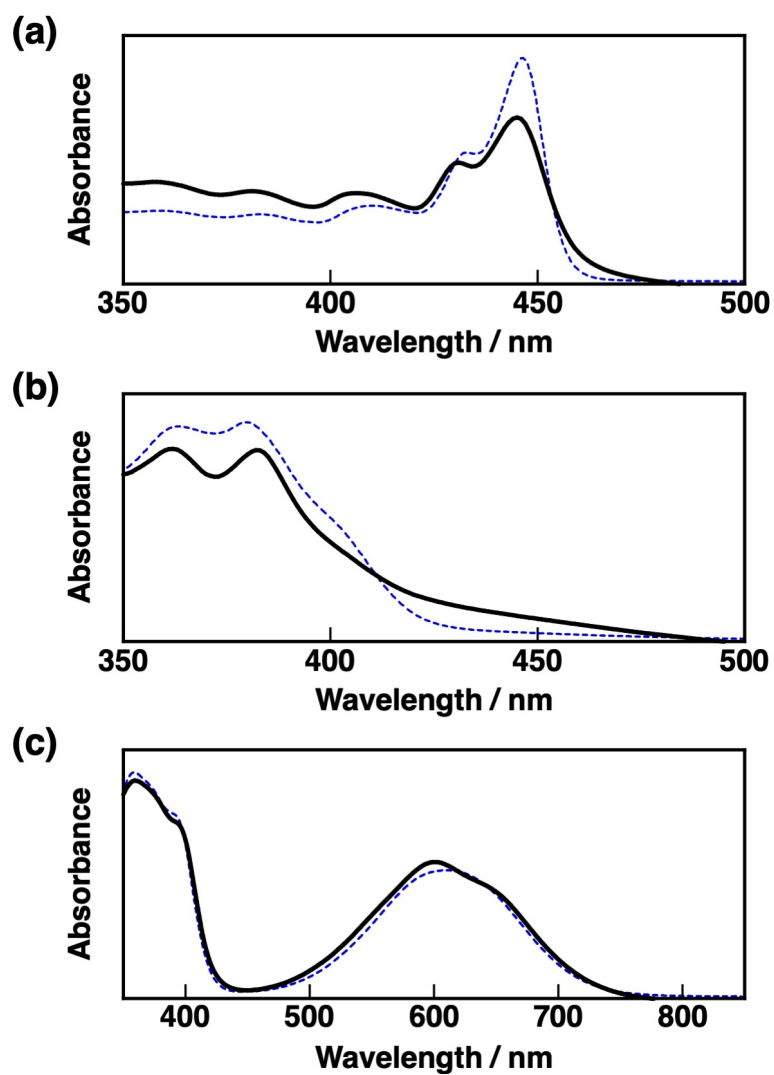


Fig. S11 Comparison of UV-vis absorption spectra of the supramolecular polymers of (a) S-NDI2, (b) ref-S-NDI and (c) S-NDI2-DEA in the MCH/toluene (4:1 v/v) solutions (blue dashed lines) and in the solid states (black solid lines).

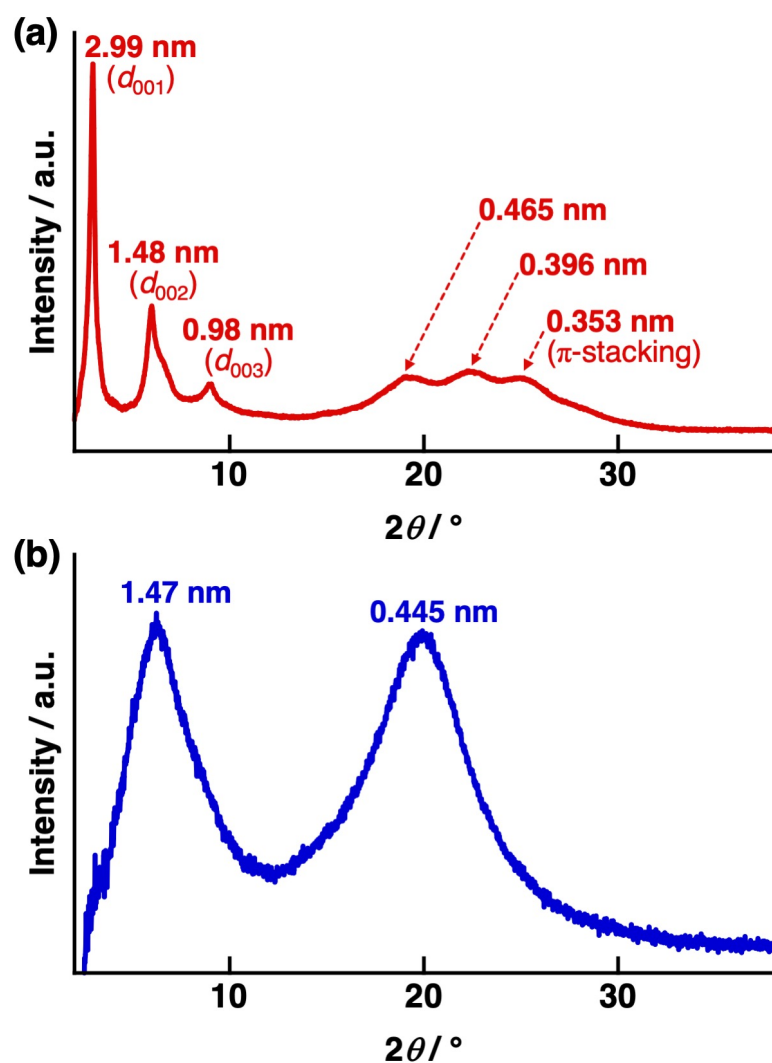


Fig. S12 XRD patterns of the supramolecular assemblies of (a) S-NDI2 and (b) S-NDI2-DEA in the solid states at 298 K. The background (non-diffractive silicon sample plate) data were subtracted from the raw data. The peak at $2\theta = 6.02^\circ$ ($d = 1.47$ nm) of the S-NDI2-DEA supramolecular assembly matches with the length of the S-NDI2-DEA along the short axis (*ca.* 1.5 nm as shown in Fig. S8g).

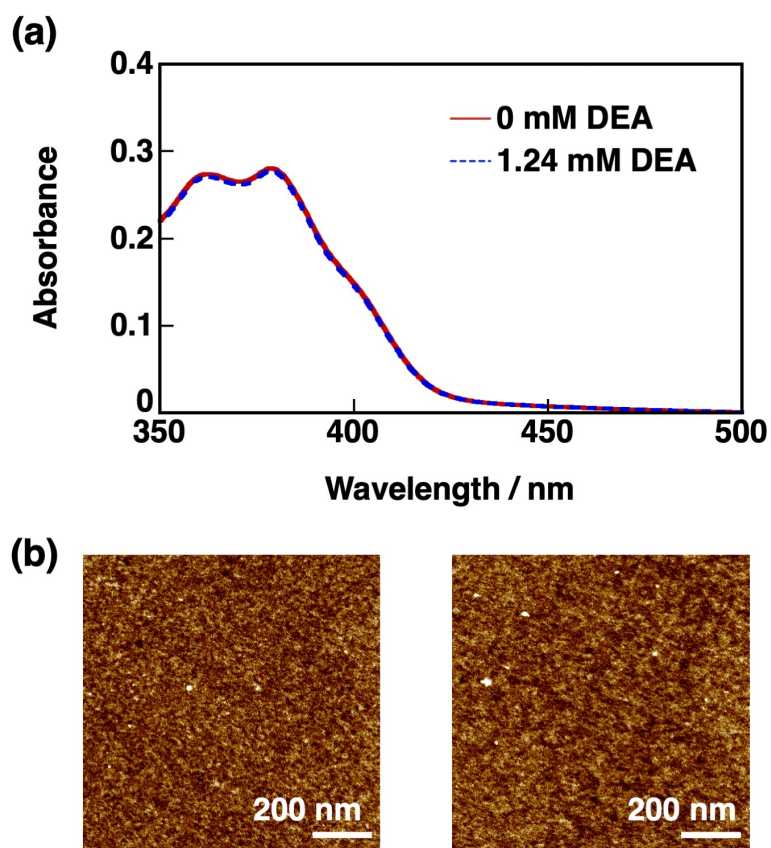


Fig. S13 (a) UV-vis absorption spectrum of the **ref-S-NDI** supramolecular assembly ($C_T = 25 \mu\text{M}$) in MCH/toluene (4:1 v/v) solvent before (red line) and after (blue dashed line) addition of 1.24 mM **DEA** at 298 K. (b) AFM images of spin-coated samples from the MCH/toluene (4:1 v/v) solution used for the UV-vis absorption measurement in the absence (left) and presence (right) of **DEA**. Scale bar: 200 nm.

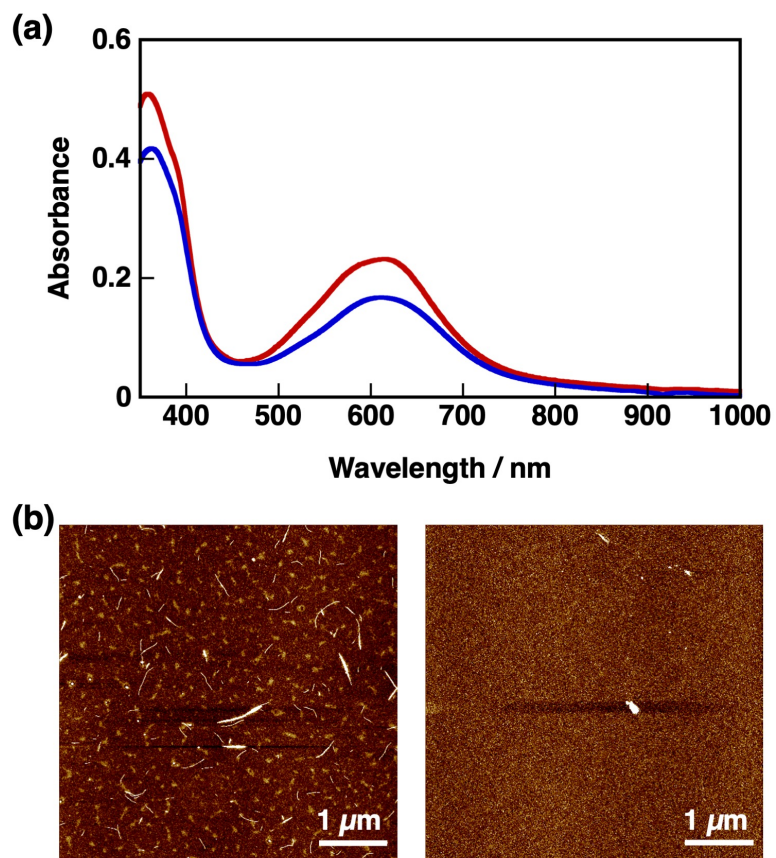


Fig. S14 (a) UV-vis-NIR absorption spectra of supramolecular polymer of **S-NDI2** 465 min after the addition of 1,4-diaminobutane at 298 K (red line) and the isolated reaction product that was cooled from 363 K to 298 K at the rate of 1 K/min in MCH/toluene (4:1 v/v) (blue line). (b) AFM images of spin-coated samples from the solutions corresponding to the red line (left) and the blue line (right) in (a). Scale bar: 1 μm .

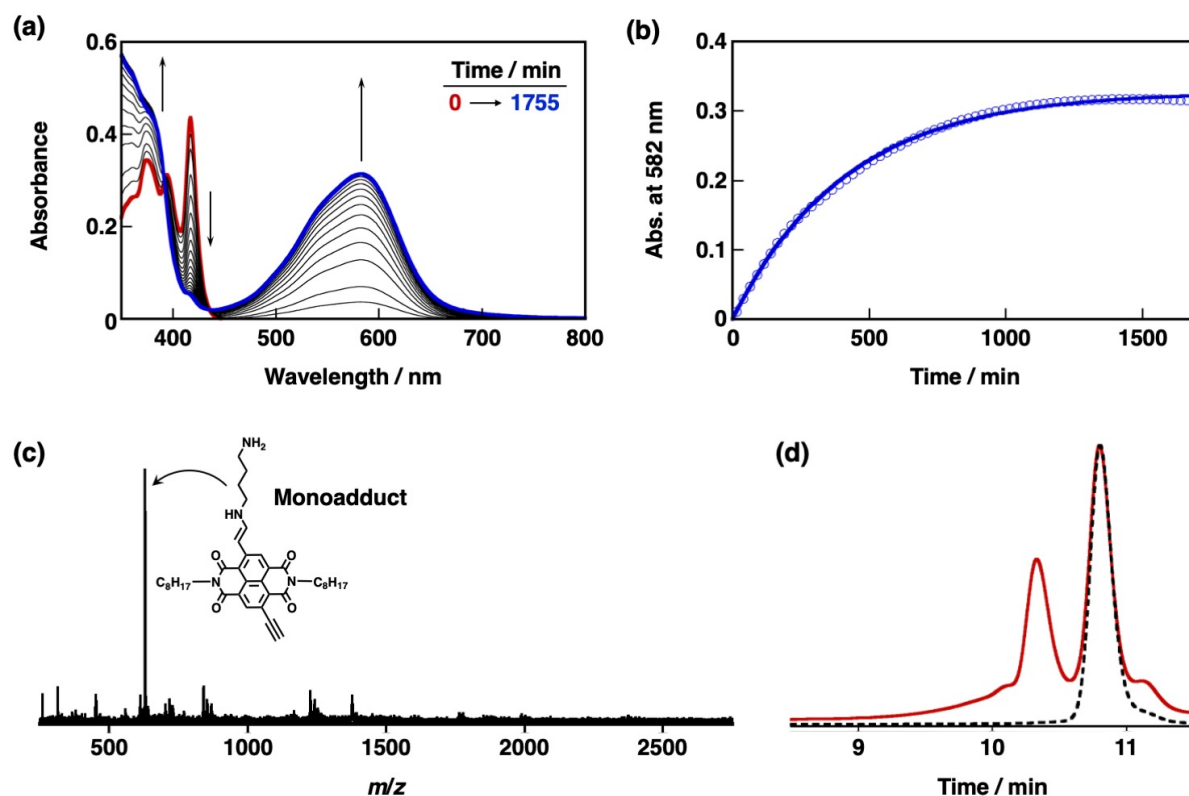


Fig. S15 (a) UV-vis absorption spectral changes of **NDI2** (25 μM) observed upon addition of 0.62 mM 1,4-diaminobutane to a MCH/toluene (4:1 v/v) solution of **NDI2** at 298 K. (b) Time profiles of absorbance change at 582 nm in the reaction of **NDI2** (25 μM) with 0.62 mM 1,4-diaminobutane at 298 K (blue circle). during the reaction, fitted by pseudo-first-order kinetics curves with an R^2 value of 0.998. (c) MALDI TOF-MS (positive ion, linear mode) chart obtained 1725 min after the reaction between **NDI2** (25 μM) and 1,4-diaminobutane (0.62 mM) was initiated in MCH/toluene (4:1 v/v) at 298 K. (d) GPC charts obtained before (black dotted line) and after (red line) the reaction of **NDI2** (1.2 mM) with 1,4-diaminobutane (1.2 mM) in MCH/toluene (4:1 v/v) for 18.5 h at 298 K. The chromatograms were normalized to the starting material (**NDI2**). The GPC charts indicate the existence of unreacted **NDI2** and an amine monoadduct only, which is consistent with the results of UV-vis absorption spectra and MALDI TOF-MS.

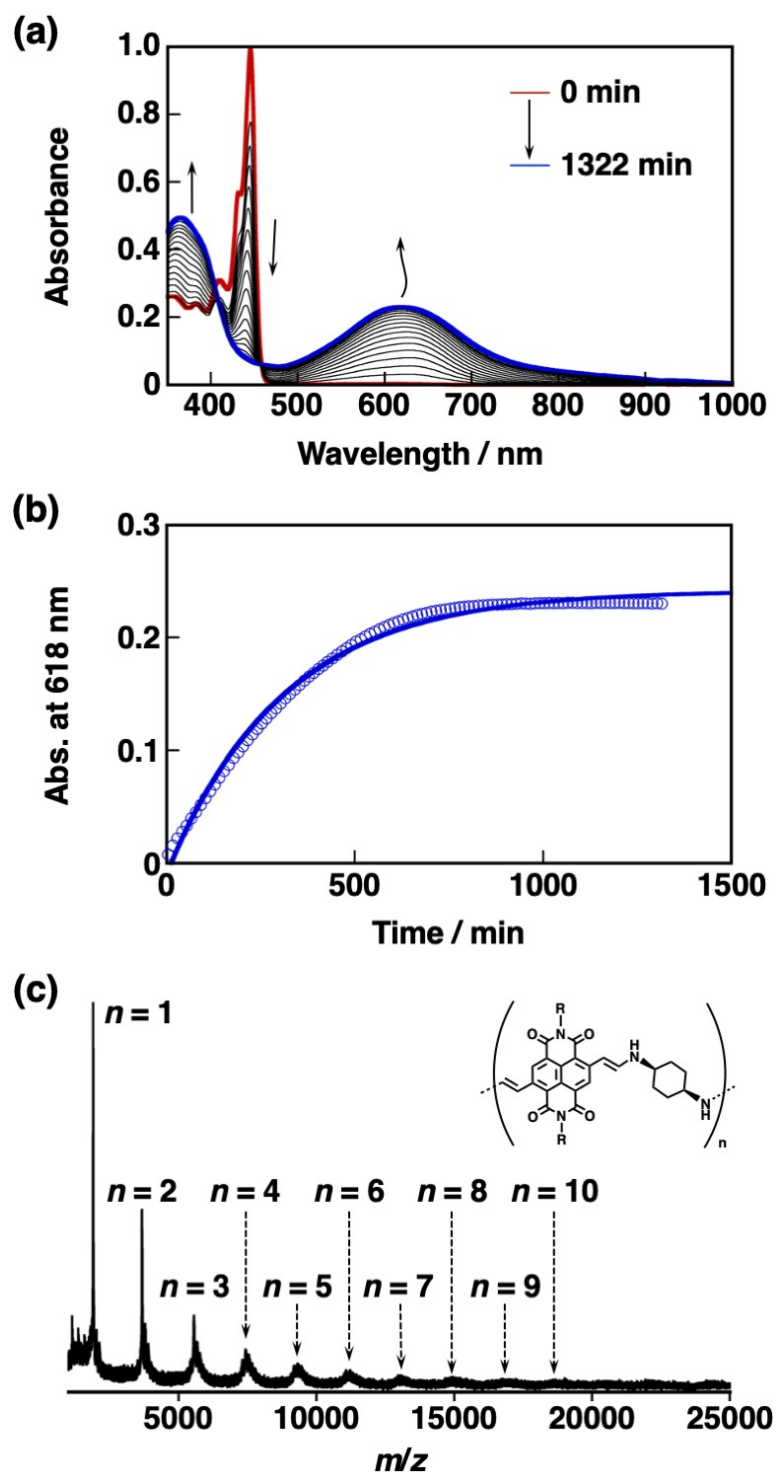


Fig. S16 (a) UV-vis-NIR absorption spectral changes of **S-NDI2** (25 μ M) observed upon addition of 0.62 mM *cis*-1,4-cyclohexanediamine to a MCH/toluene (4:1 *v/v*) solution of **S-NDI2** at 298 K. (b) Time profiles of absorbance change at 618 nm (blue circle), during the reaction, fitted by pseudo-first-order kinetics curves with an R^2 value of 0.993. (c) MALDI TOF-MS (positive ion, linear mode) chart obtained 1322 min after the reaction was initiated. Some oligomers' peaks were split into several peaks, which were assigned to the oligomers with different terminal groups, *i.e.* ethynyl and amino groups.

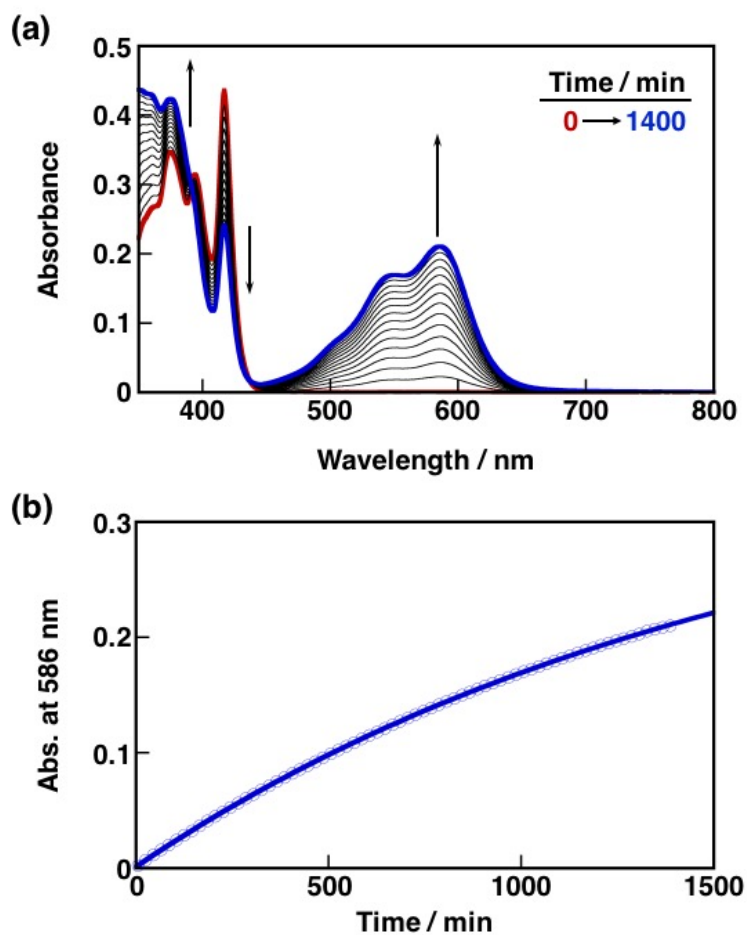


Fig. S17 (a) UV-vis absorption spectral changes observed upon addition of 0.62 mM *cis*-1,4-cyclohexanediamine to a MCH/toluene (4:1 *v/v*) solution of **NDI2** (25 μ M) at 298 K. (b) Time profile of the absorbance change at 586 nm (blue circle), fitted by a pseudo-first-order kinetic curve with an R^2 value of 0.999.

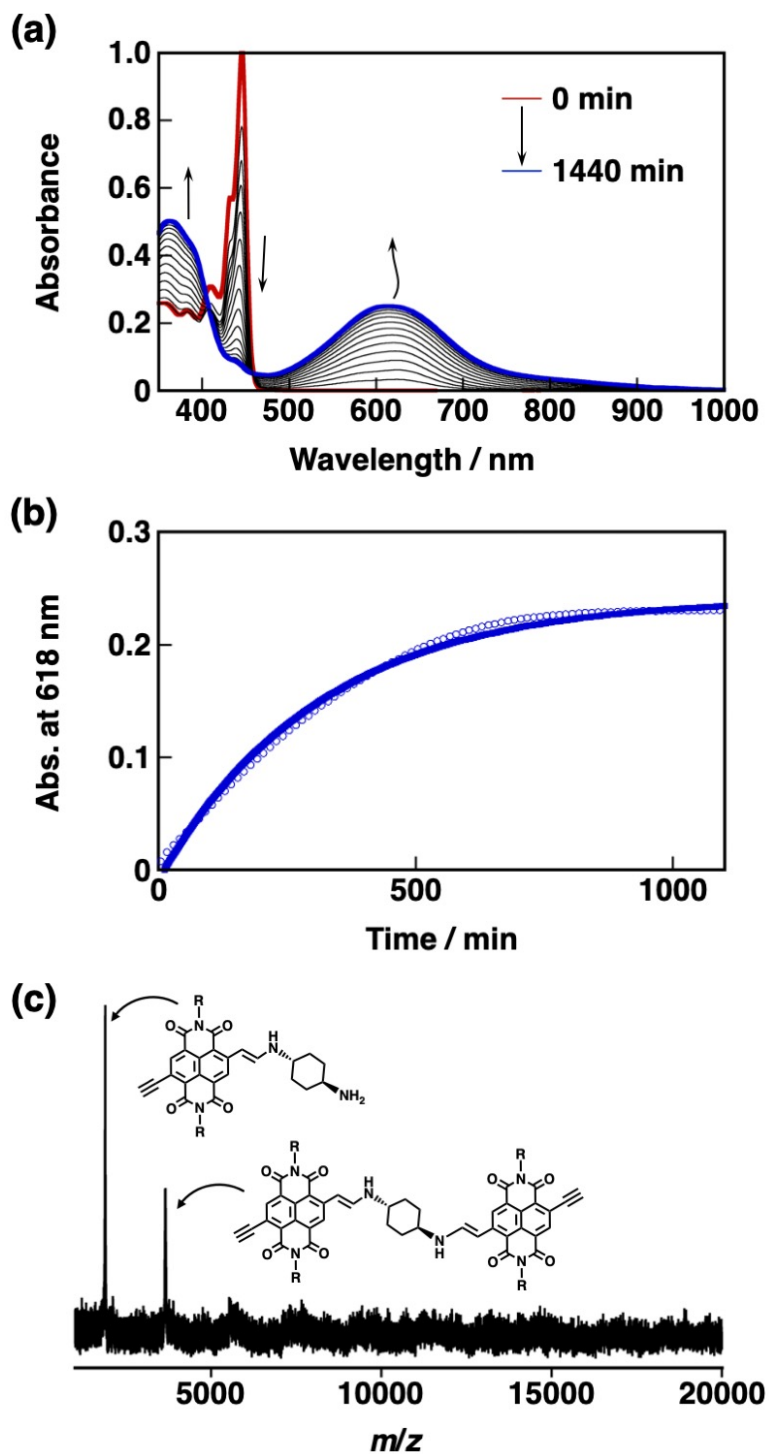


Fig. S18 (a) UV-vis-NIR absorption spectral changes of **S-NDI2** (25 μM) observed upon addition of 0.62 mM *trans*-1,4-cyclohexanediamine to a MCH/toluene (4:1 v/v) solution of **S-NDI2** at 298 K. (b) Time profiles of absorbance change at 618 nm (blue circle), during the reaction, fitted by pseudo-first-order kinetics curves with an R^2 value of 0.993. (c) MALDI TOF-MS (positive ion, linear mode) chart obtained 1440 min after the reaction was initiated.

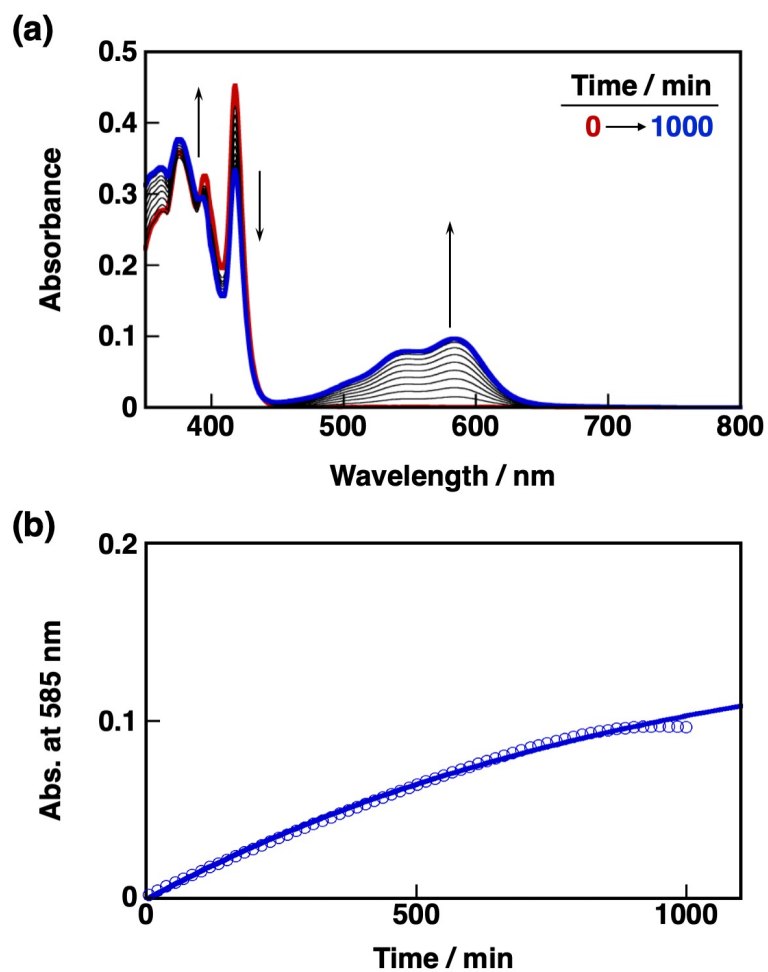


Fig. S19 (a) UV-vis absorption spectral changes observed upon addition of 0.62 mM *trans*-1,4-cyclohexanediamine to a MCH/toluene (4:1 *v/v*) solution of **NDI2** (25 μ M) at 298 K. (b) Time profile of the absorbance change at 585 nm (blue circle), fitted by a pseudo-first-order kinetic curve with an R^2 value of 0.997.

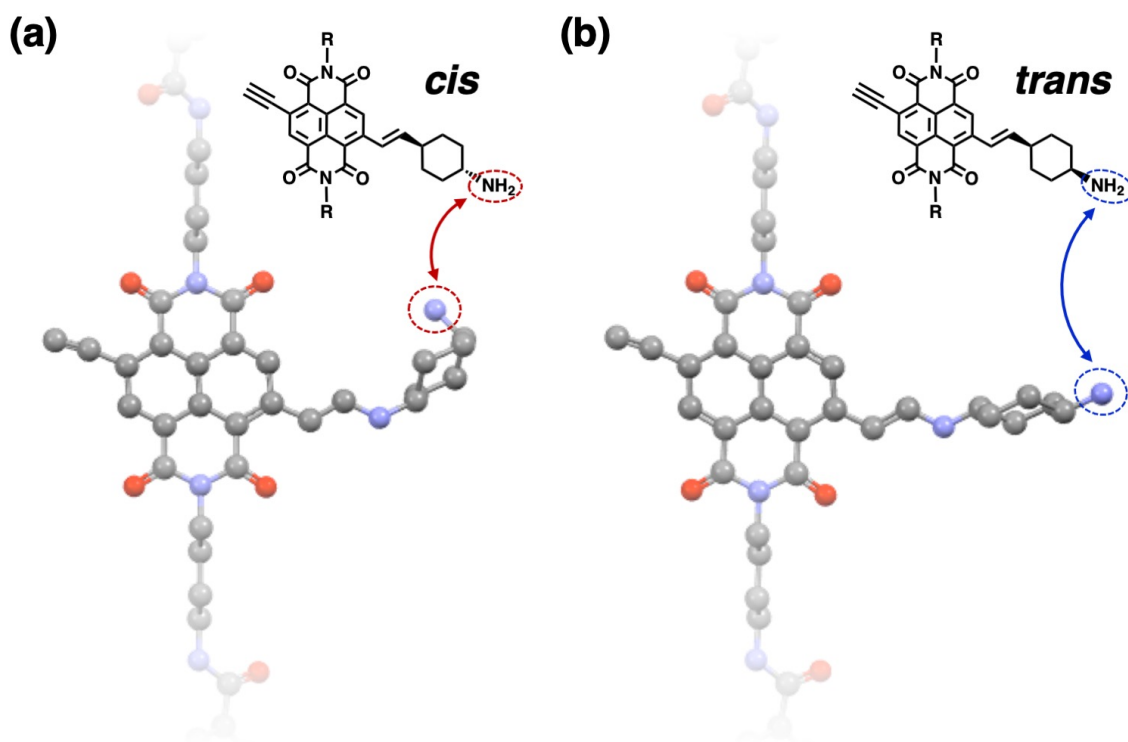


Fig. S20 DFT optimized structures of (a) a *cis*-1,4-cyclohexanediamine monoadduct and (b) a *trans*-1,4-cyclohexanediamine monoadduct of **S-NDI2** calculated at the B3LYP/6-31G* level. The alkoxy groups ($-\text{OC}_{12}\text{H}_{25}$) were substituted by methoxy group for simplicity. Hydrogen atoms are not shown for clarity.

S4. Supporting References

- S1 G. R. Fulmer, A. J. M. Miller, N. H. Sherden, H. E. Gottlieb, A. Nudelman, B. M. Stoltz, J. E. Bercaw and K. I. Goldberg, *Organometallics*, 2010, **29**, 2176.
- S2 Gaussian 09, Revision E.01, M. J. Frisch, G. W. Trucks, H. B. Schlegel, G. E. Scuseria, M. A. Robb, J. R. Cheeseman, G. Scalmani, V. Barone, B. Mennucci, G. A. Petersson, H. Nakatsuji, M. Caricato, X. Li, H. P. Hratchian, A. F. Izmaylov, J. Bloino, G. Zheng, J. L. Sonnenberg, M. Hada, M. Ehara, K. Toyota, R. Fukuda, J. Hasegawa, M. Ishida, T. Nakajima, Y. Honda, O. Kitao, H. Nakai, T. Vreven, J. A. Montgomery, Jr., J. E. Peralta, F. Ogliaro, M. Bearpark, J. J. Heyd, E. Brothers, K. N. Kudin, V. N. Staroverov, R. Kobayashi, J. Normand, K. Raghavachari, A. Rendell, J. C. Burant, S. S. Iyengar, J. Tomasi, M. Cossi, N. Rega, J. M. Millam, M. Klene, J. E. Knox, J. B. Cross, V. Bakken, C. Adamo, J. Jaramillo, R. Gomperts, R. E. Stratmann, O. Yazyev, A. J. Austin, R. Cammi, C. Pomelli, J. W. Ochterski, R. L. Martin, K. Morokuma, V. G. Zakrzewski, G. A. Voth, P. Salvador, J. J. Dannenberg, S. Dapprich, A. D. Daniels, Ö. Farkas, J. B. Foresman, J. V. Ortiz, J. Cioslowski, and D. J. Fox, Gaussian, Inc., Wallingford CT, 2009.
- S3 Y. Tang, L. Zhou, J. Li, Q. Luo, X. Huang, P. Wu, Y. Wang, J. Xu, J. Shen and J. Liu, *Angew. Chem., Int. Ed.*, 2010, **49**, 3920.
- S4 S. Ogi, V. Stepanenko, J. Theirs and F. Würthner, *J. Am. Chem. Soc.*, 2016, **138**, 670.
- S5 M. M. J. Smulders, M. M. L. Nieuwenhuizen, T. F. A. de Greef, P. van der Schoot, A. P. H. J. Schenning and E. W. Meijer, *Chem.–Eur. J.*, 2010, **16**, 362.
- S6 S. Ogi, K. Sugiyasu, S. Manna, S. Samitsu and M. Takeuchi, *Nat. Chem.*, 2014, **6**, 188.
- S7 R. B. Martin, *Chem. Rev.*, 1996, **96**, 3043.